the dozens of other hot isotopes with hard gammas has been accounted for yet, and we have only looked at three hours out of a considerable time period with southerly winds!

In fact, even Woodard himself ends up calculating 29,9 (!) mrem at Middletown. He calls this an overestimate, appearing to believe the TLD measurement.

Naturally, it cannot go without comment that the 20 TLD's were the one set of data, albeit extremely limited in scientific merit, that was completely under company control. The company and its contractors plainly must have had an interest in low readings. The evaluation procedure had to be done right. Once the crystal has been heated, the record is lost. You can't turn back to any "original data".

What really happened at TMI-2, and what were the consequences? It appears that there is hardly a compelling case so far, on the basis of monitors and gadgets only, whose readings have been evaluated by the Defendants, or whose missing readings have been interpolated somehow. So why not turn to an overwhelming body of primary evidence, namely what happened to the people and the animals and the plants and trees in the environs of TMI? We are all aware that living beings have a range of sensitivity in reacting to radiation or other poisons, and that some more care is required in collecting this evidence than clipping newspaper stories or noting down bar gossip. But the proper techniques are fairly standard, and the major pieces of this puzzle that have come to my attention so far have certainly not converted me to the myth that, let's say, TLD's are rigorous, quantitative evidence, whereas people and their observations and sufferings are secondary, "subjective", "unscientific" evidence.

1.7 The human and biological evidence

It could not be the purpose of this sub-chapter to repeat or summarize the pertinent reports and documentation of symptoms of acute radiation sickness like nausea, erythema, of immune system depression, of rare cancers, of sickness and mortality statistics, and of the characteristic damage to the leaders of Norwegian spruce and to the bark of the sugar maple. I must admit that by only reading about it I would not have been

able to grasp the compelling nature of this evidence. I am not familiar with the ways in which various people and organizations have tried to cope with the TMI issue in the past 15 years. I do know, however, that any country should encourage individuals and local initiatives who try to obtain some justice for the people brutally thrown out of their lives' tracks, and to obtain some sense of justice for the entire nation, rather than discourage them. It is an absurd notion that such a grave load of destruction and suffering, based on personal experience and observation of thousands of people, could be written off as "psychological stress". I wouldn't blame people for refusing to believe that such a massive cover-up was possible right in the middle of democratic America. But apparently the worse catastrophe of Chernobyl 1986, whose heavily contaminated plumes hit practically all European countries within a few days, was needed to reopen the TMI case.

So this last piece of the TMI puzzle should rather be the first and most important one in a country, whose admirable legacy to humanity has been the supreme right of each individual to be happy and to be unharmed.

1.8 Preliminary conclusions and proposed proceedings

If the best promise of science should be redeemed in terms of enlightenment and the pursuit of happiness, science must be absolutely free, adhering to the principles of truth and objectivity. An attempt has to be made to accept and assemble all pieces of the TMI puzzle, certainly not excluding major ones. Thus, it is clear that this treatise, concentrating on meteorological issues, will have to keep an eye on the many other scientific disciplines involved.

The scientific background of the voluminous official TMI literature has turned out to be extremely unsatisfactory, or even hostile:
Much missing knowledge has been pretended to exist, to the point of implying control of events and precision of computations, both illusory. On the other hand, much available evidence and knowledge has been left aside or dropped, if not outright suppressed.

Elementary demands of scientific methodology like cross-checking data and results for consistency (validly pointed out by R. Webb), and illustrating the sensitivity of results to realistic variation or uncertainty of parameters, have not been met.

Consider this situation:
We have a seemingly wide discrepancy between the TLD-based millirems claimed by the Defendants, and the hundreds of rems up to 1000 rems (tree damage) implied by the human and biological evidence. In trying to bridge this gap, it has been shown already that neither the assumed releases nor the TLD's are trustworthy.

I consider it my task to determine whether and how the very high doses could have been incurred - refusing to dismiss the thousands of human and other living witnesses without a further look. Clearly, all we can hope for is to establish reasonable hypotheses, as we cannot have absolute certainty or precision on most of the puzzle's parts. Quite a few building blocks will be needed on the way, meteorological considerations being one of them, the vast field of radiobiology forming many others. If we knew everything about the releases and the vagaries of wind, weather and diffusion with impossible precision - how much would we then know about real, effective doses, that is damage to health suffered by people, animals and the vegetation?

It turns out not nearly enough. Many of the not so "noble" gases and other relevant isotopes are nasty β-radiators; the pertinent official dose factor (skin and, more importantly, inhalation) upon β-submersion in a radioactive cloud of Xe-133 is almost an order of magnitude higher than the one for gamma-whole body. The activity concentration of I-131 is, fortunately, orders of magnitude less than the one for Xe-133. If it were the same, the iodine would deliver a dose ten times higher compared to the xenon on gamma-submersion, but roughly a thousand times higher on β-submersion!! Worse yet: official dose factors may not reflect the state-of-the-art of radiobiology. The physics of radioactive decay in air, of the ensuing ion clusters, possibly radioactive daughters, "mere" electrically charged atoms or chemically active radicals is bad enough, but the physics, chemistry and biology of analogous processes in human tissue is almost hopeless. Does β-radiation penetrating the

skin reach the layers where it can damage the immune system? Are the soft gammas more dangerous than we thought? Has direct deposition of hot particles on the skin ever been considered by the Defendants' experts? Or possible adsorption of ion clusters on aerosols and subsequent deposition on trees?
Apart from making brief reference to β-skin-dose and inhalation of iodine, starting from tiny concentrations and calculating tiny dose contributions, none of the above topics is even remotely covered by them, although they are the professionals who are supposed to know best. Don't they know or do they refuse to tell us?

The deficiency of the Gaussian model used and its meteorological underpinning has been stated before; it will be the topic of a part of this treatise. A further tacit model deserves attention and critique, however: Woodard vaguely implies that a TLD reading would be the dose which a person would receive if he or she stood on the receptor point naked for days on end (breathing forbidden, of course). He knows this picture to be wrong, so he does not state it explicitly. This systematic tendency to talk only about the gammas up there, forgetting the rest, goes so far as to suggest that submersion in a radioactive cloud, which you need for β-exposure, is a somehow very mysterious, rare, "unproven" event, occurring at most when a plume or puff is being mixed to the surface as a whole. This is, of course, a ridiculous contention.

Any plume, even if the maximum concentration were near the effective height of emission, reaches the ground at some concentration, depending on the stability class and the distance travelled. In stable conditions concentrations near the ground would be minute, but then, of course, the very concentrated plume may directly impinge on a slope higher up, causing the worst of β- and γ-submersion upon breathing in the radioactive gases or particles, plus skin dose plus direct deposition of hot particles!

I see my task as a meteorologist along two avenues:
First, to fill in the weather picture that is completely missing so far, to quote the most pertinent state-of-the-art flow models, in whose development, incidentally, US scientists have played a leading part, to apply them grosso modo to the extremely complicated hilly countryside around TMI, and herewith to correct wrong implications from Woodard's

inadequate model. Also, the capping inversion and other modifications of the dispersion features need to be taken into account.

Secondly, I see a definite need to work out relatively simple, straightforward graphical or tabular illustrations, demonstrating some of the more important mechanisms. This is because the Defendants along with their experts make a point of not clearly showing and explaining the elementary processes and results, their sensitivity to critical assumptions or the restrictions of the underlying models. The only graphs and tables they present are the end products of much averaging, obscurantist for the most part, as you cannot see and check the individual event (plume, puff, trajectory) any more, and you lose sight completely of the fact that a number of the most important agents has been left out altogether.
Fractions of annual MPC!
In compensation, they bend over backwards in taking note of some irrelevant detail, or in showing their consideration for the notorious individual on Hill Island.

Another Red Herring is Woodard's recent pride, the finite-plume computations of gamma-dose rate. If a computer does it, why not do it? Allright, but then it would only be fair to point out how uncertain the elements of this computation are: Releases? Exact shape of the plume? Dose buildup-approximation? TLD response? or: Damage to human tissue by the gammas?

Finally, let me deliver a note of thanks to the USA which is not without irony: Thanks for having been priviledged to live there for more than four years and to have encountered some of the finest meteorology in the world. Ironic, that I should be in a role now to contribute meteorological expertise in a country which has developed the staggering body of scientific expertise in the first place!
Another thanks from me for having been taught the admirable, democratic Anglo-Saxon tradition of expressing scientific results in common-sense terms, as opposed to the traditional German-Austrian authoritarian tendency: A professor should not be understood by the common people! And yet another irony, that, of all people, I should insist on clear, elementary illustrations of the principles at work,

being confronted with US-American experts who have visibly abandoned their own best traditions.

2. Weather, Airflow and Stability on the Regional Scale

2.1 The General Weather Situation surrounding the TMI disaster.

The general weather pattern during the decisive last days of March 1979 pretty much reflects the planetary circulation regime valid for the entire month of March, as described by Taubensee (1979), and to some extent continuing into April (Wagner, 1979). The quasi-stationary upper ridge over the Northern Rocky Mountains was displaced somewhat westward, forming a blocking structure together with an upper trough off California and Mexico (see Fig. 2.1 b). Between that and the next major planetary features downstream, i. e. a trough over the Western Atlantic linking up to a massive cutoff low over the Canadian Arctic, and the Azores high, which comes in a blocking arrangement, too, a shorter wave pattern became established, consisting of a broad upper trough over the Great Plains and a flat ridge of high pressure across the Appalachians and the Atlantic Seaboard. This regime of general westerlies with some shifts and rearrangements was largely responsible for the warmth of March experienced across much of the US, and some heavy precipitation in Midwestern states.

The first of two surface maps shown (Fig. 2.1 a), a few hours before start of the accident, with the surface high still west of the Appalachians, reflects the last surge of cold air which had invaded the northern US states between March 23/26. Soon afterward, however, the broad frontal zone in advance of the Midwestern upper trough, pathway of repeated cyclones travelling up from the Southwest toward the Canadian Great Lakes region, becomes stalled in the right position to the rear of the Appalachian upper ridge to cause massive advection of warm and humid air from the Southwest towards the Northeastern states. Within the 2 1/2 days following March 27 19 EST, the entire troposphere in the region of concern up to more than 10 km height becomes warmed up continuously, the lower levels up to 800 mb (2000 m a. s. l.) by $\approx 20\,^{\circ}$ C!

This general regime of warm air advection remains responsible for heavy rains and flooding across the Southeast far into April. In and around Pennsylvania cooler temperatures return by April 2, following a first weak cold front on March 31, but the southerly regime is not conclusively terminated until April 5/6, when a severe near blizzard-type storm sweeps across the Great Lakes area, with northwesterly winds to the rear of the cold front and trough gusting up to 40 knots even at Harrisburg. The pertinent planetary wave features remain displaced eastward during April, as compared to March.

The second surface map shown (Fig. 2.1 b) already represents the beginning of strong warm air advection with southerly winds between the surface anticyclone, which, by now, has shifted eastward across the Appalachian mountains to eventually join up with the Bermuda high, and lower pressure across the Midwestern plains. The first hours into the accident happen to coincide with the transition between the two surface maps shown. At 04 E. S. T. the surface high is located right over the Middle Susquehanna Region. Surface winds turn from westnorthwesterly clockwise to northerly, northeasterly, easterly and southeasterly (see Fig. 2.3).

At this point we show two consecutive soundings from Washington D. C. (Fig. 2.2) to give the reader an idea of the vertical structure of the atmosphere. The first one, taken on the late afternoon of the accident day, has the cooler "old" airmass well-mixed up to = 1200 m a. g. by insolation on this perfectly clear day. As it has become warmer already on the Western and Northwestern Plateau around Pittsburgh, this pool of cool air, as yet higher than the mountain crest height, tends to flow westward, seeping across mountain passes and general regions of lower terrain. This configuration (Fig. 2.1 b) has a striking resemblance to the weather map accompanying the "shallow foehn" across the European Alps: Cyclones tracking along the Bavarian foreland = Northwestern Plateau; cool air forming a wedge of high pressure across the Po valley = Pennsylvania and southern foreland east of the Appalachian mountains, draining into the Northern Alpine forelands across mountain passes. We will see that such foehn effects on the Western slopes of the Alleghennies are apparent on March 28. Without much theory the figure makes it almost evident how the warm air advection beginning from 850 mb (= 1500 m a. s. l.) on up has put a lid on the atmosphere.

Whereas warmer (= lighter) air below colder (= heavier) air would result in violent vertical mixing, i. e. thunderstorms and tornadoes, in the extreme, warm air on top of cool air, called "inversion", suppresses vertical motion, and, in due course, horizontal air flow as well, since the latter is rarely possible without the former.

The sounding 12 hours later has the very strong inversion nearly touching the ground, i. e. less than 400 m a. g.. This might look like the result of subsidence (see sub-chapter 2.3), but the occurrence of precipitation makes it unlikely. Neither could the apparent warming during the night hours have been caused by solar radiation. Therefore, warm-air advection at rather low levels is the only remaining candidate. In accordance with what was explained above, then, the vertical structure of the lower atmosphere upstream of TMI had become one of extreme stagnation beneath an almost suffocating formidable inversion during the night 28/29 March. The sequence of hourly weather events and winds at Harrisburg (Fig. 2.3) demonstrates how on days two and three (March 29/30) winds dropped to very weak and variable, with near calms for hours in a row.

By comparison, the severity of stagnation may be illustrated by the mean wind speed at Harrisburg in March, which is quoted as being = 10 mph or 9 knots!

Ironically, then, the balmy weather in the course of the decisive first few days after time Zero turned out to be, in a sense, worse than snow storms, floods or tornadoes, as regards atmospheric dispersion. As the warm air advection has finally penetrated the very lowest atmospheric layer close to the ground during March 29, the grip of inversion = stable stratification begins to loosen, and by March 30 record-high temperatures are reported from the Middle Atlantic states (Washington, Baltimore). Winds, however, still remain generally weak until April 5.

Beyond the foregoing broad description of events, unfortunately, analysis becomes very involved. The structure of the frontal zone ahead of the broad trough across the Western and Midwestern USA is quite complicated, as indicated by the waviness up to the 500 mb-level (Fig. 2.1 b) and by inconsistencies in the various published surface analyses (Deutscher Wetterdienst).

Advances of the warm air from the southwest come in surges spacewise and timewise. Warm-front waves, notorious for their treacherous nature, propagate along the frontal zone, which lies almost parallel to the upper-level flow. As if this were not enough, the course of weather events is affected also by boundary layer processes in the lowest kilometer or so (daily march of insolation, friction), and by the position and shape of the Appalachian mountain relief. For a really satisfying analysis, these various contributions should be understood and sorted out. Three-hourly surface and 12-hourly 850 mb-maps have been reanalyzed in detail.
I defer the presentation and discussion of these maps to subchapter 2.4. The rewarding additional insights to be gained therefrom, relevant to the consequences of the TMI disaster, will be apparent. These analyses set the scene for investigating the smaller-scale flows in chapters 3 and 4.

2.2 Data sources, discussion of scales

Both surface and upper air data are needed for a fair description of the synoptic weather situation. We have used official NMC weather maps of the National Weather Service (obtained from the National Climatic Data Center, Asheville, N. C.), surface and 850 mb, including three soundings from Pittsburgh, Pa., Washington D. C. and Albany N. Y. with significant levels, from March 28, 1979, 00 GMT (Greenwich Meridian Time, currently called UTC = Universal Time Coordinated) = March 27, 19 E.S.T. (Eastern Standard Time) through April 2.

The surface observations and maps are done at 3-hourly intervals, with a station density of roughly half a dozen across Pennsylvania, for example. Upper-air soundings, on the other hand, are launched only once every 12 hours at stations several hundred km apart. The idea is that thermal and flow structures of the "free atmosphere" are much smoother than near the surface, and, in any case, leave enough "signals" in the surface observations, such that upper-air synoptic features can be resolved in sufficient detail timewise and spacewise by "building upwards" from the comparatively dense surface observation network. The concept of space-time consistency is essential in this process, and the use of the hydrostatic law and certain quasi-equilibria. Some techniques and examples will be given later, as needed, along with the proper notation.

Fortunately, the NMC analyses contain the original observations, otherwise a reanalysis could not be done. The NWS should be commended for being able to furnish this high-quality information in very well readable form 15 years after the event. TV viewers may be surprised to learn that satellite pictures are NOT the backbone of synoptic analysis and weather forecasting.

In an attempt to secure all the available relevant weather information in the regional vicinity of the TMI plant, records of hourly surface weather observations from more than two dozen airports in Pa., Md. and De. between March 27 and April 2, 1979, were obtained from the National Weather Service. 20 of these report 24 hours around the clock. These valuable data include temperature and dew point, wind direction and speed, altimeter setting and often other forms of air pressure, total sky cover, various cloud levels, visibility and weather phenomena like rain or haze. The average distance between these major regional airports is still on the order of 50 to 100 km. They tend to be located on higher ground, which is good for their being representative of the general surface flow in the area. Clearly, however, we have no chance of finding local flow features of any kind in these data or any other, although the badly convoluted topographic relief and the prevailing condition of quasi-stagnation and extreme thermal stability are highly conducive to locally disturbed, variable wind flow.

This gap will, to some extent, be closed by the results of a numerical flow model with a grid resolution of 5 x 5 km horizontally and down to 20 m vertically (see chapter 3).

Regarding even smaller-scale features like flow around individual hills, turbulent wakes, impaction on hill slopes facing the TMI vent stack and many others, we are left with pointing to a large body of theoretical, numerical, experimental (wind tunnel) and empirical results (special field studies) on what is likely to happen under various circumstances. The cases shown can only be exemplary - an exhausting treatise of all possibilities would be far beyond anybody's reach. An illustration of plausibility is what has been done (see chapter 4).

2.3 Notation

I will use certain expressions and variables, not all of which can be explained in detail. They will be for the benefit of meteorologically trained readers, but I will make every effort to explain the essence of things in terms as simple as possible.

I will keep the treatise as brief and readable as possible. Graphs and analyses in this chapter will be either copied from official publications, or hand-drawn. Computerized graphs would only make sense for large numbers of the same kind. In our case, there would be no gain other than possibly the illusion of perfection, only considerable labour and costs incurred.

All times will be converted to local time = E.S.T. There is a five-hour time difference between GMT, used worldwide in the Met. Services, and E.S.T.

00 GMT ⟶ 19 EST of the previous day
12 GMT ⟶ 07 EST of the same day.

28/16 will mean March 28, 16 E. S. T.

Wind direction is the direction from where the wind blows:
A south wind or southerly wind blows from the south. This is contrary to oceanographic custom:
An "easterly current" is heading towards the east!

Wind speeds are given in knots:

1 kn = 0.515 m/s = 1.15 mph = 1.853 km/h.

All official weather maps, surface or upper air, use flag symbols as follows:

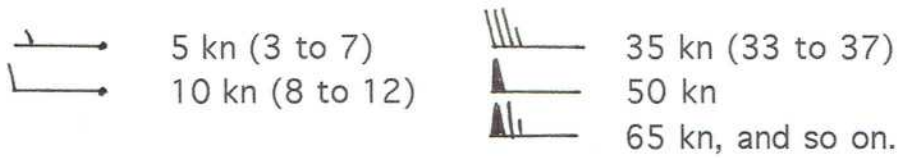

However, for some representations of surface winds (e. g. Fig. 2.3) we will conveniently use a wind scale five times more sensitive.

Wind may also be given in terms of its horizontal components u in the x-direction (positive from west to east) and v in the y-direction (positive from south to north), or, alternatively, in vector notation

$$\mathbb{v} = (u,v)$$

For dynamical considerations we also need the vertical wind component w, positive for upward air motion and negative for downward ("subsidence"). Although only on the order of cm/s and thus far from being observable directly, w is highly significant in terms of weather phenomena.

Actual temperatures t and dew points are expressed either in ° F or in °C:

°F	5	14	23	32	41	50	59	68	77	86	°F
°C	- 15	-10	- 5	0	5	10	15	20	25	30	°C

Absolute temperature T in ° Kelvin is = t (° C) + 273.16.

A very fundamental property of actual temperature is that an individual air parcel's temperature is NOT being conserved when it moves around. Rather, the parcel cools by 1 ° C per 100 m of vertical rising (working against the earth's gravity like a mountain climber) and warms by 1 ° C per 100 m of vertical sinking. This is why meteorologists have defined a fictitious quantity called "potential temperature" Θ which is being conserved under the above premises.

Θ is highly useful for theoretical considerations and in practical applications. I only note here a handy approximation according to Steinacker:

$$\Theta \approx 273.16 + t\,(°C) + \frac{z}{100} + \frac{1000 - p_o}{12.5} \qquad (2.1)$$

where z is station elevation in meters,
the denominator 100 reflects the abovequoted 1 ° C per 100 m, and p_o is pressure reduced to sea level in millibars (see further down).

One could say that Θ serves to make temperatures at different elevations easily comparable. For example, when the lowest layer of the atmosphere is well-mixed due to solar heating of the soil, the air temperature will decrease with height by 1 ° C per 100 m, whereas Θ will be constant in that layer (see Fig. 2.2). Moving away from that extreme state, actual temperature, as a rule, will decrease by less than 1 ° C/100 m (see upper part of Fig. 2.2), or it may even, over a limited height interval, increase with height, an "inversion" of the ordinary, average state (compare also Fig. 4.1)!

From (2.1), potential temperature Θ will, at most, be constant or otherwise always increase with height z, if we stay in the same place horizontally. Thus, the atmosphere at level z_2 higher than z_1 will rarely be actually warmer than at the lower level, but will practically always be "potentially" warmer.

All this is related to the fundamental property of Θ. Now, if there is sinking air motion ($w < 0$) and you feature yourself, say, sitting on a

mountain observatory, the actual temperature t there will increase, the more so, the faster the environmental potential temperature Θ, as measured, say, with a balloon sounding, increases with height. This latter quantity, in mathematical terms $\frac{d\Theta}{dz}$ or, more connotatingly,

$$N^2 \equiv \frac{g}{\Theta} \cdot \frac{d\Theta}{dz}$$, where g = 9.81 ms^{-2} = acceleration of gravity,

is the concise expression of THERMAL (STATIC) STABILITY of the atmospheric layer in question: +)

The larger $d\Theta/dz$, the heavier the penalty on vertical motions, organized or turbulent.

The larger $d\Theta/dz$, the more will atmospheric layers stacked on top of each other tend to behave and move in a disconnected way, decoupled from each other. An "inversion" (large $d\Theta/dz$) in a basin will act like a lid, preventing the volume of air below from mixing or exchanging with outside air, thereby, on occasion, causing severe accumulation of air pollution.

Another significant quantity that is being conserved along an individual air parcel's path = "trajectory" is the specific humidity q (grams of water vapor per kg of air). This is true in the absence of condensation or evaporation. As warm air masses are practically always humid air masses, q is a most useful additional "tracer" in our case.

Air pressure p is expressed either in mb (millibars), now preferably called hPa (hekto-Pascals), or in inches:

1 inch = 33.8642 mb

Since pressure is the weight of an air column per unit area, it decreases so markedly with elevation that this amount of decrease per 100 m, namely $\approx$ 10 mb, is no less than typical horizontal changes of pressure over, say, 1000 km!

Pressure, then, has three uses:

1 as an approximate height scale (see Fig. 2):
If we talk about 850 mb-maps with temperatures, winds and so forth, we talk about values at an elevation of $\approx$ 1500 to 1550 m a. s. l.

+) Modifications due to saturation with respect to water vapor will not be discussed here.

2. as an integral "signal" of the temperature structure above the observation point: warm air is relatively lighter (by a few percent), cold air is heavier.
Despite a lot of "compensation" occurring in the atmosphere, resulting surface pressures, for example, may vary by, say, 10 % worldwide (see Figs. 2.1 a, 2.1 b).

3. as horizontal differences of pressure or "pressure gradients", which act to initiate air motions = winds.
Any air parcel tends to flow from higher to lower pressure, but then it may get deflected by the earth's rotation or by additional forces. In order to correctly isolate these relatively minor, but dynamically all-important horizontal pressure gradients from the overwhelming vertical pressure gradient, which cannot be as such released to drive air motions, measured pressures p must be "reduced" to some uniform elevation. Customarily, this reference elevation is mean sea level z = 0, and a fictitious atmosphere must be assumed when "reducing" station pressure hydrostatically to sea level.

NMC synoptic surface maps use the actual station temperature in the pressure reduction procedure, but at airports the "standard atmosphere" is used instead in computing the "altimeter setting" or QNH. The merits of either approach cannot be discussed here in detail.

Rather than looking at the variations of pressure across a level surface, it has become standard practice to equivalently plot the undulations of an isobaric surface.

Temperature advection

When the expression "warm air advection" or "cold air advection" is being used, it means horizontal advection.
Plainly: If temperatures 100 km to the southwest are warmer by 2 ° C and the wind blows exactly from there to here at 8 m/s, temperature here will increase by

$$\frac{2\,^{\circ}C}{100\,km} \cdot 8\,\frac{m}{s} = 16 \times 10^{-5}\,^{\circ}\,C/s = 7\,^{\circ}\,C \text{ within 12 hours,}$$

as long as no other warming or cooling process comes into play.

We have learned before that sinking motion in the vertical direction ("subsidence") always raises the actual temperature and viceversa. More generally, if we were to sit in a particular fixed location, any elevation, and if we or an instrument experienced, say, the temperature rising locally, this can have one of three causes:

1. Local heating, most typically by insolation
2. Warm-air advection
3. Subsidence

As a rule, of course, two or all three of these mechanisms will act simultaneously, and not necessarily all in the same direction. There could be enough sunshine to cause local net warming despite cold-air advection, for example. Or, rather typically, warm air advection would be associated with rising motion, such that the net temperature change would still be positive, unless the evaporation of falling precipitation would bring the temperature down again. The afternoon of March 28 happened to be a period when all the three mechanisms worked in the same direction.

In principle, horizontal temperature advection can be determined, but the problem remains of how to relate momentary values to averages over 12 hours or over layers in a situation where the advection occurs in individual surges, as mentioned before. Also, in this situation of strong inversion, weak winds and additional topographic blocking it becomes doubtful whether certain balances are attained well enough to make analytical use of them.

Lastly, a related topic is recognizing inversions genetically. In a "subsidence inversion" potentially warmer and very dry air is "imported" from above, such that temperature will increase locally, but specific humidity q will decrease. A "frontal inversion", which reflects warm air advection, may descend to lower levels much like a subsidence inversion temperaturewise (see the example in Fig.2.2), but, in contrast, specific humidity is very high above the inversion, as the warm air being advected is generally also very moist.

2.4 Detailed Synoptic Analysis for March 28 and 29

In summary, the evolution of temperatures, winds, weather and atmospheric stability can reasonably be understood in terms of two "warm fronts" progressing across the region of interest from the

southwest and being stalled on their way later on. This double structure is apparent in the data; it is also very plausible as the overall temperature difference across the frontal zone is quite large. We will see that the warm fronts stretching over more than 1000 miles are not straight lines on a map, but that the warm air advection comes in individual surges or "tongues", partly because the cold air being replaced offers more or less resistance to the oncoming warm air masses. Generally, warm air on top of colder air is a very "stable" configuration, as discussed before, so warm air has a hard time gradually "eroding" the cold air from above, especially if the latter is dammed up and thereby "protected" by a mountain range. In addition to this deformation of the warm fronts seen on maps (Figs. 2.5 and 2.6), the frontal zones become "disfigured" within the lowest 1 km or so above the ground by the daily march of temperature, heating at daytime and cooling at nighttime. Given these caveats, I still consider it useful to give the reader a highly idealized picture of these two frontal zones, looking at them sideways from the southeast, as if they were undistorted planes. They separate three air masses, which I call cold, moderate and warm. Typical daytime temperatures at the lower elevations would be in the forties, upper fifties and lower seventies, respectively, with an additional general warming of up to 10 ° F by March 29 and 30 outside the Canadian cold core mass. "Moderate" could be "warmer" or "cooler", depending on the sense of progression of the fronts. For interpretation of the lines of equal potential temperature Θ = isentropes shown in Fig. 2.4, suffice it to say that along each horizontal surface, the changes of actual temperature t are a perfect echo of the changes of Θ, the amount of change being slightly less by a few percent.

Thus, within each air mass, horizontal temperature differences ("gradients") are relatively small; these gradients become concentrated within the "frontal zones" shown. The same is true in the vertical direction, only that here we must talk about potential temperature, to be correct, rather than actual temperature. The "frontal inversion" marks a region of strong increase of Θ with elevation z, a very stable region, that is.

On weather maps, for clarity, the intersection of a frontal zone, typically only 50 to 100 km across, with a surface of constant height or constant pressure is drawn as a mere line.

The general sense of progression of the two warm fronts from the southwest towards the northeast is indicated by thick arrows. It should

The southern tongue has moved across the southernmost strip of Pennsylvania during the night March 28/29. This tongue, due to "conditional instability" released by forced ascent, will give rise to frequent rain showers, even some thunderstorms, shifting from Indiana and Ohio on the afternoon and evening of March 28 across eastern Pennsylvania and on to the Atlantic coast in the early morning hours of March 29.

The northern warm tongue will be even more active in this respect: The shores of Lake Erie and Lake Ontario experience rain showers, as well as parts of Illinois, Indiana and Ohio from the forenoon of March 29 all the way through March 31, when the cold front finally crosses Pennsylvania in the afternoon.

The rain showers, normally quite suspect in a warm sector, might mislead the inexperienced also by the evaporative cooling of the air they cause. We think, however, that it would be exaggerated to interpret these features as a "cold front", even if they are actually accompanied by slight cold-air advection.

The two tongues are seen to be drifting backwards toward the south at a later stage. This is in response to the general southward drift of the cold front/occlusion, pushing the conveyor belts ahead of it. Very significantly, the two tongues miss a region between them, which happens to include a part of Pennsylvania. We will pursue this feature and its consequences on the surface maps.

Fig. 2.6 a:
Isochrones of the first warm front at the surface. Times in E.S.T.. Frontal symbols as standard. The cold front/occlusion to the NW is only indicated. See text.

Fig. 2.6 b:
Isochrones of the second warm front.
Not all dates are entered, as the front lines may be either too close to each other, masked by nocturnal inversions or otherwise not identifiable.
The cold front/occlusion to the NW is entered fully, with an indication of where the first warm front joins it. See text.

Investigating the displacement of the surface warm fronts next (Figs. 2.6 a, 2.6 b), a "steering" action by the warm-air tongues described above will be apparent, including even steering of the first surface warm front by the second warm frontal zone lying on top of it (compare Fig. 2.4). The coupling of near-surface and upper-air thermal and flow features is, of course, a necessity in a fluid continuum. The exact description, not to speak of explanation, may be quite difficult. The waviness of the westerlies at, say, 500 mb was noted before. It would only be natural to expect that gentle troughs and ridges there would be associated with the warm tongues shown at 850 mb. The "hen and egg" problem of which comes first is a moot question. For the purpose on hand, we are surely justified in restricting our analysis mostly to the layers 850 mb and below.

Pursuing the first surface warm front (Fig. 2.6 a), it appears to leap forward at times, e. g. between 28/10 and 28/13. This is, of course, mostly not kinematic propagation, but a reflection of the fact that a shallow nocturnal inversion, which had made the edge of the warmer air at the surface stay far towards the southwest, is being "burnt away" by insolation. In such daytime conditions, the second surface warm front almost catches up with the first, such that a large temperature contrast may occur between the cold and the (very) warm air masses across a small distance.

For example, on 28/19, Huntington, W. Va., reports 70 °F, Cleveland, Ohio, only 46 °F. Similarly, Evansville, Indiana, has 70 °F, St. Louis, Mo., 73 °F, but Green Bay, Wisconsin, only 37 °F! The US surface analysis at least shows a warm front between these stations, but the global surface map of the German Weather Service for the same date (28/19), which has a selection of these and similar stations plotted, shows them all in one warm sector without a single front in between, indicating once more the confusion of analyses!

At a later date, 29/10, Morgantown, W. Va., near the southwestern corner of Pennsylvania, reports 73 °F, but (Penn) State College, a mere 200 km to the northeast, 47 °F!

The first warm front pushes ahead towards the SW corner of Pennsylvania late in the afternoon of March 28, staying behind both to the west, over Illinois, Indiana and Ohio, and to the east. Here, the surface high is centered right over the Harrisburg area at 28/04 (= time Zero), drifting off toward the eastsoutheast thereafter, but the relatively shallow cool air dome (Fig. 2.2), which is deeper further north (compare Figs. 2.7 b and 2.7 c), is still pushing southward along

Fig. 2.8 a affords a comparison between the official NMC surface analysis and our own detailed analysis. The latter brings out the tight packing of the isobars across the Appalachians, their distinct "bulge" westward beyond Northwestern Pennsylvania, suggestive of both the above mentioned "shallow foehn" and a tendency for stagnation west of Harrisburg, and the highly characteristic deformation of both warm fronts.

Fig. 2.8 b, in its upper part, illustrates the tropically warm conveyor belt, reaching northward from the Gulf and splitting up into tongues. On arrival in Pennsylvania, this air is, of course, still very warm, but it has been cooled somewhat on its way by contact with the cooler ground and by upgliding at upper levels. The overall temperature and humidity contrast amounts to fifty degrees Centigrade! The "polar front" would be delineated roughly by an equivalent potential temperature of 35 °C. The detail Fig. 2.8 b, lower part, merely serves to illustrate the tendency for stagnation to the W and N of Harrisburg, as expressed by the widening contour lines and consequent slackening winds.

Fig. 2.8 a:
Surface maps, March 28, 1979, 19 E.S.T.
Upper part: NMC surface analysis with station reports
Isobars every 4 mb.
Lower part: Own detailed analysis
Isobars every 1 mb
Two surface warm fronts entered.
Map section exactly as upper part. See text.

Fig. 2.8 b:
850 mb maps, March 28,1979,19 E.S.T.
Different map scales
Upper part: NMC analysis with station reports and contours, contour interval 30 m. Equivalent potential temperature plotted (°C), interval 4 °C.
Lower part: Detail
Contour analysis at intervals of 10 m using heights and height gradients from observed winds.
Absolute contour height = 1457 m + DP.
Stagnation tendency shown (see also detailed surface isobars in Fig. 2.8 a).

Fig. 2.9 illustrates the widespread near stagnation across Eastern Pennsylvania and the warmer temperatures and continuing southwesterly winds further south. An analysis of temperature maxima across Pennsylvania from the US Climatological Data revealed some maxima differing by more than 20 °F between nearby stations on March 29, but also on March 28 and 30. Some of those are very suggestive of pockets of cold air overrun by the warm air just a bit higher up, but it is too difficult to subtract out instrument errors without knowledge of the location and quality of the many lower-class stations.

We will see shortly that the second warm front didn't change that picture - in fact, it didn't even make it to Harrisburg (Fig. 2.6 b). Thus, for example, cities like Williamsport, Wilkes-Barre and Albany, N. Y., didn't experience the passage of either surface warm front, remaining in the shallow cool air throughout. In addition, any transport of air from the Atlantic would bring cool air at this time of the year (see the shape of surface warm fronts figs. 2.6 a,b). At upper levels, however, the warm air did come through, as shown, e. g., on the time-height-section Fig. 2.7 c, where the frontal inversion stays aloft.

The cooler air ahead (to the north) of the stagnating warm front across southeastern Pennsylvania should flow across gaps in the Appalachians with an easterly wind component, heading towards Buffalo, N. Y., or so. Conversely, wind flow behind the front tends to be from the southwest, rising and heading towards the N. Y. City area. By March 30 the first warm front is no longer recognizable on the maps.

For the three nearby radiosonde stations, time-height-sections have been constructed, plotting isolines of Θ = isentropes (Figs. 2.7 a, b, c). The idea is to make use of the high spatial resolution in the vertical and of the high frequency of surface observations in order to obtain a consistent picture of the evolution of temperature with time at the various elevations: If done correctly, the transition between the relatively smooth synoptic trends at upper levels and the distortions forced by the daily march of temperature in the planetary boundary layer should emerge clearly.

At Pittsburgh and Washington both warm fronts came through. Looking at the respective figures 2.7 a and b from behind, i. e. with the time axis inverted, amounting to the very rough approximation of a "frozen" spatial structure being advected by a uniform wind, one might get the idea of a remote similarity with the highly idealized structure of Fig. 2.4, although the complications of real nature will be appreciated.

The correspondence between these sections and the frontal analyses is excellent, to be sure. Take, for example, Pittsburgh: The first warm front has come close to the city by March 28/19 E.S.T., but it has not passed the station until March 29/04 E.S.T.

The passage of the second warm front at Pittsburgh between 29/10 and 29/13 (Fig. 2.6 b) is not quite so striking on the section Fig. 2.7 a, but the return of cooler air from the west between 29/13 and 29/16 certainly is, as the warm-frontal wave has propagated east, leaving Pittsburgh in the "moderate" air again. In this case, at this time of the day, there is no mistaking the cooler air and accompanying inversion for an action of local nighttime cooling, but in other cases the distinction between a nocturnal inversion (see Figs. 2.7 a, b, c for examples) and a frontal inversion near the ground may be difficult.

It has been repeatedly noted that the second warm front (Fig. 2.6 b) has many features in common with the first one. Bringing warmer air still, it has an even harder time replacing the cooler surface-based air. In fact, only the southern branch coupled with the southern conveyor belt seems to have been able to touch the ground. Blocking by the Appalachians, even retreat of the warm front during the night March 28/29 seems to work much like with the previous front, which remained quasi-stagnant in the same general area.

Across Illinois and Indiana, however, the second warm front, in retreat, already gives way to cooler air.

A new feature has been noted already: The warm-frontal wave, which carries extremely warm subtropical air towards the SW corner of Pennsylvania by 29/10 and even up to the shores of Lake Erie by 29/13, propagating further east thereafter, but not reaching Harrisburg any more. Even Washington D. C., which has been overrun by the very warm air and has experienced near record temperatures on March 30, appears to have suffered a return of some cooler air later that day.

In summary, Harrisburg has seen the (moderately) warm surface air only in a rather brief "window" during the early afternoon hours of March 29, thereby having the thermal stratification changed from "extremely stable" to "stable" between the two warm fronts. These fronts have approached each other closely in the course of the afternoon and have become quasi-stationary across southeastern Pennsylvania, with pressure gradients vanishing almost completely.

Although only 100 miles further south, Washington is already in the very warm air since the late forenoon of March 29, and the inversion has been broken there.

Thus, the Washington sounding is, unfortunately, not representative of the more stable lowest atmospheric layers near Harrisburg, a fact whose detrimental consequences for the dispersion of TMI releases must be kept in mind.

Looking at Fig. 2.6 b, the cold front/occlusion approaches Pennsylvania from the northwest across the Great Lakes late on March 29. Accordingly, this frontal system begins to push the two warm fronts back southward again, such that Harrisburg and neighboring airports to the north experience somewhat cooler air flow from the north between 29/16 and 30/00 (see Fig. 2.3), whereas light southerly to southwesterly winds at temperatures 10 ° F higher continue to blow at Baltimore, Washington and further south. At this point, it is evident from Fig. 2.6 b that a wave has formed in the late evening of March 29 along the northern cold front/occlusion, which has begun to set warm air in motion across the Great Lakes from the southwest, preventing the occlusion from hitting Pennsylvania. There follows a period of extreme stagnation across eastern Pennsylvania including Harrisburg, with many hours of calm between 30/00 and 30/16, roughly, and temperatures climbing up to the middle seventies at Harrisburg in the afternoon of March 30, and into the eighties further south. Only then the winds begin to respond systematically to the newly approaching wave, with southeasterlies turning to southwesterlies by 31/00, dropping to near calm again soon afterward until 31/08.

Later in the day, a pre-frontal squall line followed by a cold front passes through the area, initiating a slow cooling trend.

Winds drop to light and chaotic thereafter once more for more than 24 hours, until late on April 1 rain sets in ahead of a massive new wave approaching from the southwest, and winds at Harrisburg pick up speed at southeasterly direction until noon of April 2. The see-saw continues for another three days, with light and variable winds and some more rain, as stated in sub-chapter 2.1, until the long regime of general upper warm-air advection along the broad Midwestern frontal zone, with its concomitant pronounced inversion and stagnation conditions, is finally ended by the passage of both a cold front on late April 5 and the main upper trough on April 6.

Because of the general notion that the first few days after time-zero were the critical ones in terms of releases, and for reasons of economy, we have presented detailed analyses only for those days. From the general course of events it should be evident that a number of additional critical and very interesting episodes could have been chosen and analyzed in a similar spirit, up to April 5. We trust that the reader will have gained a reasonable understanding from the material presented here.

3. A regional numerical model for transport and dispersion

3.1 Choices - why to do what?

Clearly, available synoptic meteorological observations cannot determine the flow field and dispersion characteristics down to a scale of hundreds of meters or a few kilometers, as needed to estimate local transport and diffusion from TMI releases. They can, however, set the scene for the application of various techniques to be discussed in chapters 3, 4 and 5.

Neither can on-site observations on a tower be assumed to be valid out to 10 km, even 50 km, and for all heights that come out to be relevant (see 5.2).

So why not straightaway model the flow numerically using the power of modern computers? Let me remind the reader of the enormous complexity of such a task. Transport and dispersion models exist to the hundreds, many of them in the nuclear industry or in the scientific "grey zone" around it (e. g. the ARAC code). Even to list the respective acronyms would fill pages.

Quite a few of these models are global in scale, and some apparently have succeeded in simulating the path and contaminating action of the Chernobyl clouds reasonably well, after years of tuning and verification on the many observations available. They have a resolution of a few hundred km. Depending on the type of problem, other models have been designed with higher resolution, but necessarily limited domain (LAMs = "Limited Area Models").

They need information from a larger-scale model as boundary values, or else they would soon be exposed to uncontrolled "outside intervention". The most popular solution to this is "nesting" a higher resolution model domain within the next larger domain. The smaller the scale, the harder model verification becomes, as there are fewer and fewer data available.

I have had the opportunity to appreciate some of these problems talking to colleagues (Tafferner, personal communication on MM5 model, Ulrich, seminar at the University of Munich on RAMS model). The Regional Atmospheric Modelling System demands at least a year's work by a very experienced person to know what he or she is doing.

The basic prognostic equations are few and more or less the same everywhere, but there are literally thousands of "switches" in such a model for a host of empirical parameterizations of radiation and heat fluxes, friction and other boundary layer processes, surface properties, the water cycle, cloud physics and so forth. Resolution is supposed to be amazingly flexible, from 100 km down to 100 meters (!) in repeated nestings, but parameterizations may not be so flexible, interacting occasionally in an uncontrolled, even destructive way. Obtaining the boundary input can be quite cumbersome.

Documentation is a problem, as well as the need for special graphics and internal routines, or compatibility of various computer languages. Not all applications have been successes (Mursch - Radlgruber, personal communication).

It was my judgement, therefore, not only that it did not seem feasible to obtain access and results within a limited time span and financial frame, but that relatively simpler, well-tested, more robust and accessible models might be just as good, even preferable. This may appear to do injustice to the more than 50 man-years' expert work condensed in this enormous structure. There is no doubt that each of these models is capable of computing flow structures very suggestive of real nature, but I couldn't convince myself that the enormously increased expense would bear a sound relation to similarly improved results.

A similar comment might apply to a model structure like FLOWSTAR (Riddle and Staples, 1992), which purports to compute a 3-dimensional flow field and turbulence field over complex topography, into which clouds of particles are being advected and dispersed in due course.

There are, of course, a good many dispersion models which avoid the labor of computing a three-dimensional, time-dependent flow field first, but rather rely on an assumed wind field (e. g. observed or "mass-consistent" diagnostic), with the field of turbulence empirically estimated somehow. Then they pour tens of thousands of "Lagrangian particles" into this flow, following their trajectories and finally computing concentrations of effluents by counting particles per volume. However, diagnostic wind fields, as a rule, rely on too little physics and too few observations to be a dependable tool.

With a view on the short-range impact of TMI releases on the nearby hill slopes and valleys, one might think of flow simulations either with a very fine-scale model like LES (= Large Eddy Simulation), or with

laboratory experiments in a wind tunnel or in a water tank. Both techniques are valuable for demonstrating and visualizing a range of possibilities. Quite a few of the idealized results quoted in chapters 4 and 5 will be based on such techniques. However, wind tunnels are more typically used for simulating homogeneous flow with wake effects around building structures; water tanks are suitable for stratified flow, but a 1 : 1 correspondence with air flow cannot be obtained even for the most elementary dimensionless parameters, so the results remain qualitative, wind engineering still being "more an art than a science" (Meroney, 1990, p. 171).

And fine-scale numerical models remain questionable, if for no other reason, because their results cannot be any better than their input in terms of initial conditions, boundary conditions and physical parameterization. In sub-chapter 5.1 model validations will be quoted for a comparatively simple situation: stationary boundary layer, terrain flat or at most gently rolling, constant rate of emission. The sobering results should guard us against exaggerated claims.

A major part of the explanation for this failure might be that nested models driven by well-verified synoptic-scale analyses can furnish surprisingly realistic smaller-scale features, apparently even regional precipitation (Schaer, personal communication), as long as the features we are looking at do not depend strongly on the very empirical and questionable parameterization of boundary layer physics.

3.2 The model

The numerical model chosen has been developed and is being run by Dr. D. Heimann, Prof. G. Gross and Dr. J. Graf ("AMBIMET"). We have a domain 300 x 300 km in the horizontal, with 60 grid points 5 km apart in each direction. The model is therefore a regional one, not designed to simulate local flows on the scale of hundreds of meters. Arbitrary mountain topography may be prescribed at the lower boundary, as well as surface properties (here: Woods are assumed above 200 m a.s.l.). The earth's rotation is included. The model should basically be able to simulate the response of, say, very stable flows running up towards the Appalachian mountain slopes in the presence of many extremely complicated ridges, hills and valleys, whose influence on the flow cannot be studied and understood in isolation. Also, the model should show whether orographic waves forced by upper winds blowing across a part of the Appalachian ranges have any significance in our case. Thermal wind systems forced by the daily cycle of temperature are also within the model's capabilities, being still essentially hydrostatic.

The vertical coordinate is a terrain-following "sigma", with 20 grid points in a flexible resolution arrangement, from 20 m near the surface to 1.5 km from 4500 m on up. The evolution of three-dimensional, time-dependent flow is being computed, with a physics package including radiation and heat balance modified by a "screening factor", and boundary layer processes including turbulence.

The model, of course, needs proper synoptic input:
Initial profiles of temperature and wind, and later on "geostrophic winds" at two levels, say surface and 850 mb, prescribed at suitable time intervals throughout the simulation. Thereby, a large-scale temperature advection (see 2.3), warm or cold, is imposed on the regional flow. Additionally, a large-scale vertical velocity can be prescribed, which reflects convergence or divergence "known" and imposed from outside, and which acts in addition to the velocities computed by the model itself. The disturbances produced can leave the domain through "open boundaries" sideways or at the top.

The fact that the model has a horizontally uniform current impinge on the mountain relief makes for comparative ease of prescribing the synoptic input. The price to pay is the fact that the large-scale temperature advection can only be constant with height. This is sometimes an unrealistic feature, whose consequences must be studied in preliminary tests and, if necessary, mitigated by suitable adjustments.

The imposed large-scale horizontal uniformity should hardly be a problem. For example, Pittsburgh had warm-air advection already on March 28 07 E.S.T., when Harrisburg (Washington) still had cold-air advection. Being interested in the paths of TMI-releases, we clearly must choose synoptic conditions east of the Appalachians as model input.

Finally, "puff" releases, each marked separately, can be simulated, introduced at arbitrary times, locations and heights. The respective particle clouds are being traced throughout the flow in Eulerian mode, and concentrations are shown on the plots. The spatial resolution is, of course, limited by the grid resolution at all times.

Model output is very convenient and flexible. Examples will be presented in the following and in chapter 6. It should be understood that only a few examples can be documented in this report to keep it readable. The entire output is, of course, available upon request.

Fig. 3.1 shows the model's computational domain, 300 x 300 km. At this point, wind fields will be illustrated at two heights and two times only, all the rest being deferred to chapter 6. The wind fields in Fig. 3.2 are relatively uniform on this scale, horizontally and vertically, as there is still a near-mixed layer. The apparent convergence of winds from southeasterly to southwesterly going westward reflects the turning of the general winds from southerly to westerly as one moves to higher ground (compare Fig. 2.2). Surface winds are slowed by friction. Thermally driven flows are not conspicuous, and probably shouldn't be.

Seven hours later (Fig. 3.3), the "geostrophic forcing" by the synoptic pressure gradients is still pretty much the same, but the flow pattern has changed drastically as a consequence of stagnation in this very stable airmass running up towards the Appalachian hills. Over Cumberland County to the west of Harrisburg the winds have turned easterly following the pressure gradient (high pressure to the southeast), being blocked by the Blue Mountains.

Surface winds are chaotic in the TMI area. Further east, to the windward side of the ridge between Harrisburg and Reading, winds at 50 m a.g. appear to be hardly influenced by stagnation, at least as far as wind direction is concerned, whereas winds at 10 m a.g. surely are. A similar pattern is seen over the near SW of TMI, but in other regions the 50 m level has been seized by the stagnation process also. This much is likely to be realistic: Observed winds do turn easterly in the course of the night March 28/29 (see Fig. 2.3), and similar flow patterns with reversed flow at the lowest levels have been observed, for example, in conditions of stagnation over the Italian Po Valley, with foehn winds blowing on top. However, there is no way to interpret all the overwhelming detail in such maps, or to verify or falsify it, or to look at the millions of numbers, temperatures, winds at all levels evolving in time, which a numerical model grinds out.

For contrast, it should be remembered that these two figures are not representing the worst of calm winds and general stagnation yet, although the stagnation over Cumberland County on March 28/29 may well have been the worst in terms of health consequences.

Fig. 3.2:
Computed wind field for March 28, 1979, 19 E.S.T
Only a small part of the computational domain is shown.
North as in Fig. 3.1.
Upper part: 50 m above ground level
Lower part: 10 m above ground level

0.5 1 5 m/s

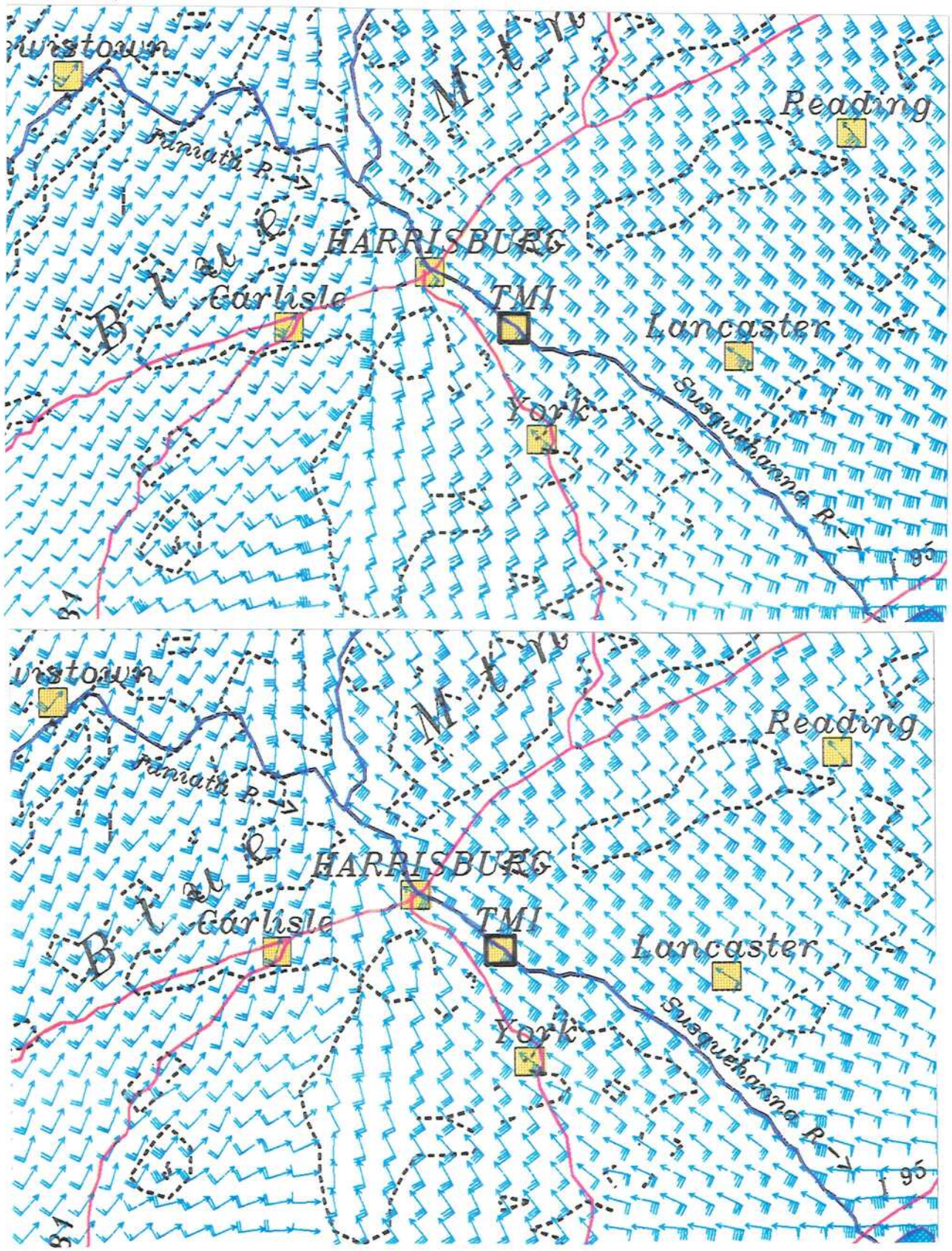

Fig. 3.3:
Computed wind field for March 29, 1979, 02 E.S.T.
Upper part: 50 m above ground level
Lower part: 10 m above ground level
See text and Fig. 3.2.

0.5 1 5 m/s

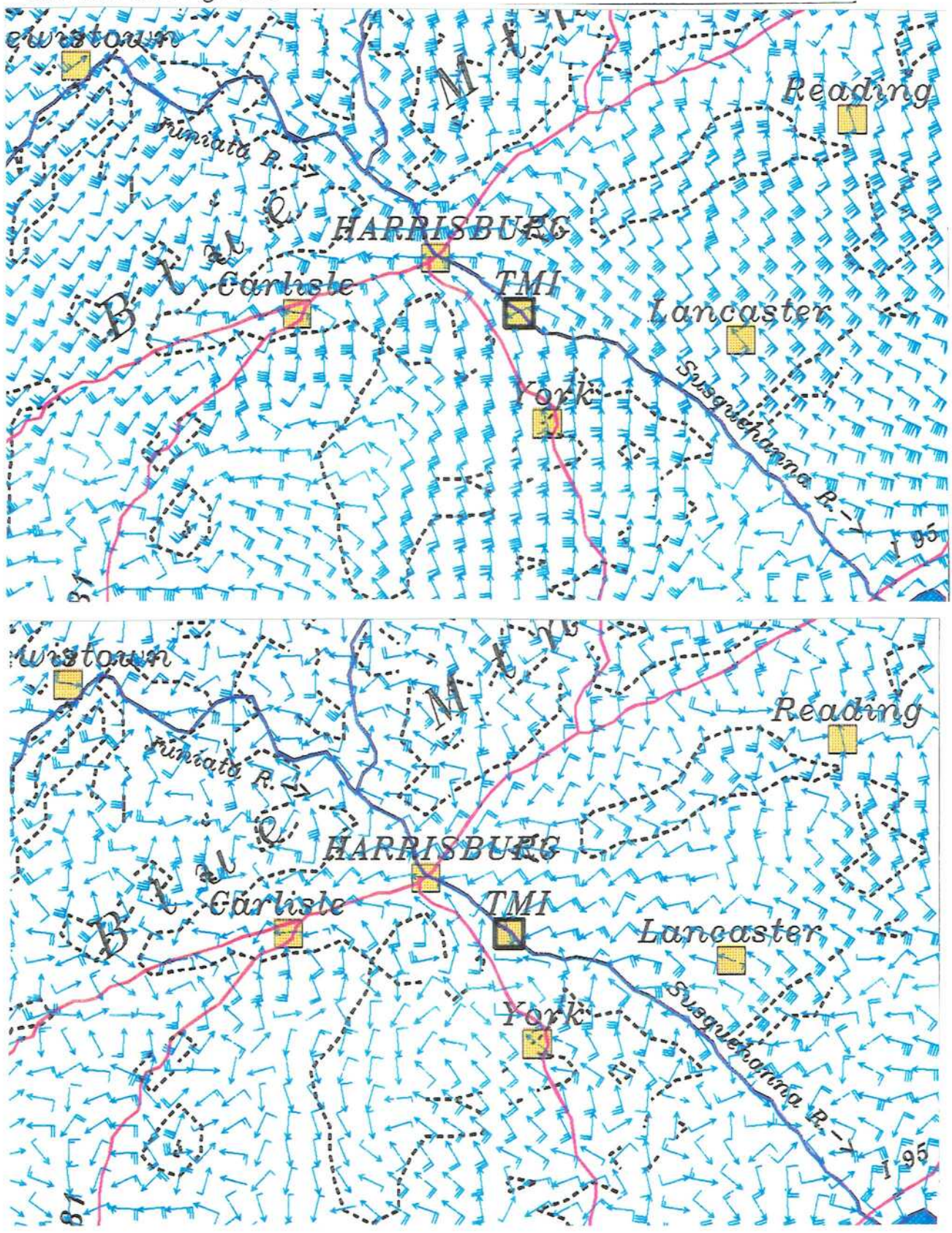

4. Airflow on the local scale

This is a vast and complex topic. An attempt must be made to bring some order to the chaos, in the sense that some of the exemplary possibilities will be shown in a very idealized fashion. Not the least of my intentions is to destroy the illusion that perfect description or even forecast of such features was possible. Insights come from a variety of techniques:

- Laboratory experiments in wind tunnels and water tanks
- Theoretical considerations
- Organized field observations
- Many recent numerical model studies
- Ballooning, paragliding, hanggliding.

The limitation of this chapter should be well understood:
Horizontal scales larger than a few kilometers are not addressed here - pertinent flow phenomena are mostly left to the numerical model and discussed there, as the need arises. "Airflow on the local scale" has the influence of obstacles in mind. To the extent that certain flow patterns occur over flat terrain also, they may be found in the discussion of boundary layers (chapter 5).

"Potential flow" is no more than a remote "ideal" in geophysical applications. This is due to complicating forces, among them friction and buoyancy forces. The latter is all-important in our case, which is dominated by inversion conditions = strong "stratification" (chapter 2, particularly 2.3). The quantitative expression for this "static stability" is (see 2.3)

$$N = \sqrt{\frac{g}{\Theta} \cdot \frac{d\Theta}{dz}}$$

This stability measure N may be more or less uniform, as in most laboratory experiments and theoretical and numerical models, or it may be concentrated in one or more shallow, strong inversions, as e.g. on the afternoon of March 28 (see Fig. 2.2). Both types, as expressed in vertical temperature profiles, are illustrated in the following Fig. 4.1:

There is not a whole world of difference between the two types, as far as overall flow properties are concerned (There is, as far as turbulence and dispersion in the lowest layer is concerned - see chapter 5). We get some approximation to "homogeneous" flow (negligible buoyancy) in the limit of the inversion either becoming weak and/or moving further up and away, strong enough winds, and the hill extending $\approx$ 1 km in the horizontal direction or less, as shown schematically in the following

Fig. 4.1:
Temperature profiles of lower atmosphere, schematic. See text.

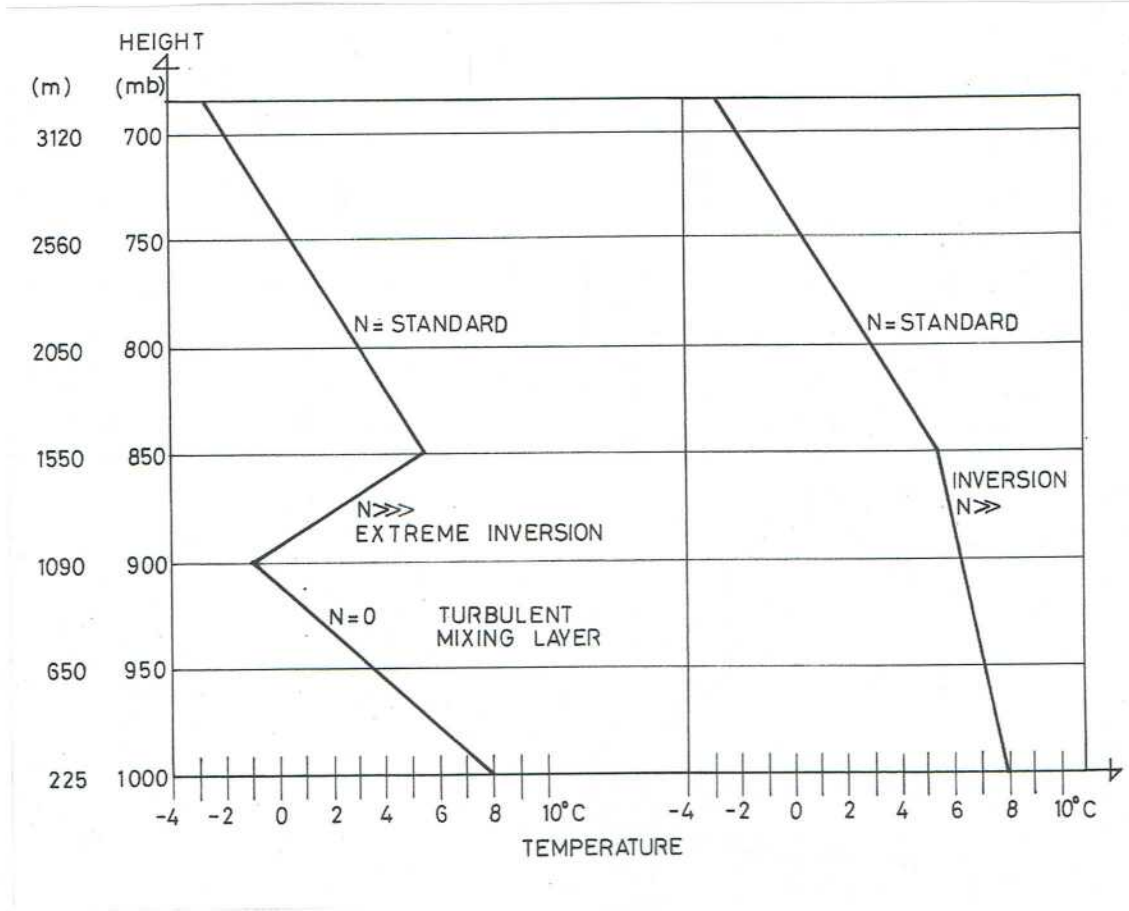

Fig. 4.2 a. This figure and some more are drawn two-dimensionally for easier visualization - the real world is three-dimensional!

The flow in Fig. 4.2 a is still not quite potential flow, certainly not in the lee, where the boundary layer adhering to the hill surface loses momentum because of surface friction and separates, reattaching soon again in this case. In purely potential flow the streamlines and the pressure distribution would be perfectly symmetric, with no net drag force on the obstacle.

Favorite places for observing such frictionally modified flows have been relatively smooth hills like Askervein hill in the Outer Hebrides

and Brent Knoll in Somerset. Here, the flow pattern is rather independent of wind speed, as it should (Mason and Sykes, 1979).

Fig. 4.2:
Schematic flow patterns, side views.
4.2 a and b: *Homogeneous flows with friction*; 4.2 b: *steeper hill side.*
4.2 c: *Stratified flow over a mountain ridge.*
For description see text.

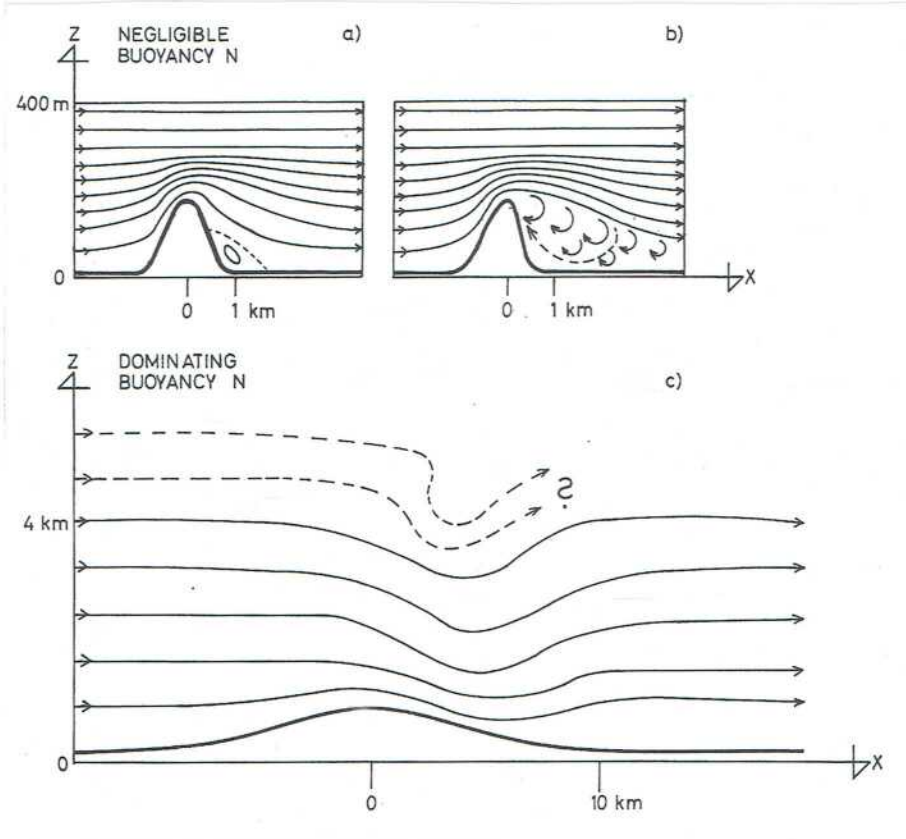

A large separated "wake" or "cavity" region with weak, but distinct recirculation is shown in Fig. 4.2 b. Such a pattern is likely to occur on slopes steeper than ≈ 1/3 or with sharp edges, projecting corners or sudden roughness changes or the like. The transition to separated flow is very sensitive. When it occurs, however, it dramatically changes the effective shape of the obstacle and the distribution of pressure everywhere. The cavitation zone may suddenly break down on a slight change of the oncoming wind direction or turbulence intensity or overall pressure field, and be reestablished just as quickly.

The strong wind shear at the wake boundary constitutes an unstable vortex sheet, which tends to roll up into turbulent wake eddies. The flow streamlines may not reattach out to a distance of ≈ 20 times the hill height.

Fig. 4.2 c is shown only for contrast: from now on we consider flows with the effects of stratification dominating. The particular sketch is the extremely schematic flow over a mountain ridge of extent ≈ 10 km. The streamline pattern is highly assymetric, with strong foehn-type winds blowing down the lee slopes. Recalling Fig. 4.1, a gross difference would be that with more continuous stratification (right picture) gravity wave energy can radiate freely upward, whereas an elevated strong inversion (left picture) tends to trap vertical wave propagation, thereby approaching a "shallow-water"-situation, with possible hydraulic jumps and rotors. Breaking waves (top of Fig. 4.2 c) can occur in both uniform and layered media.

In the following we investigate flows over and around topographic features of smaller horizontal extent, namely in the km-range. There are four good reasons for this:

- During the days of concern, wind flow at crest height of the Appalachian ridges was more parallel than normal to those ridges.

- If and when forced currents as in Fig. 4.2 c had nevertheless occurred in places, the numerical model (chapter 3) should capture them.

- We are mostly interested in flow features in the near vicinity of TMI.

- Flows like in Fig. 4.2 c under variable conditions like hill shape or different wind and temperature profiles are a vast topic by themselves.

At this point, I refer to the most useful compendium "Atmospheric processes over complex terrain" (Blumen, ed., AMS 1990) to keep the quoted literature at a minimum. This book has a lot to say on all the topics in this chapter.

By conventional wisdom, it might seem that the effects of stratification N tend to disappear when the hills' extent shrinks to ≈ 2 km or less. However, the dividing streamline concept, originally proposed by Hunt and Snyder (1980), has shown that the massive disturbances suffered by a very stable flow over and around obstacles

depend to a large extent on obstacle height (see below), but little on its exact shape or horizontal extent.

The remainder of the chapter will be devoted to this highly applicable, if pragmatic flow model. Three chapters in the abovequoted book make ample use of the dividing streamline concept:

Chapter 5: by D. J. Carruthers and J. C. R. Hunt

Chapter 6: by S. R. Hanna and D. G. Strimaitis

Chapter 7: by R. N. Meroney

Figs. 4.4 and 4.5 together should give the reader a fair idea. Air flow is from the left at speed U in both figures.

Its stable stratification is quantified by the buoyancy frequency N, typically $10^{-2}s^{-1}$ or somewhat more. Hill height is = H.

The all-important dimensionless number here is the Froude number

$$F = \frac{U}{N \cdot H},$$

from which the height of the dividing streamline H_c may be estimated as follows:

$$H_c \approx H \,.\, (\,1 - F) \qquad \text{or} \quad H_c = 0, \text{if } F>1 \qquad 4.1$$

and the flow over and around the hill may be described in terms of four different regions with the aid of H_c.

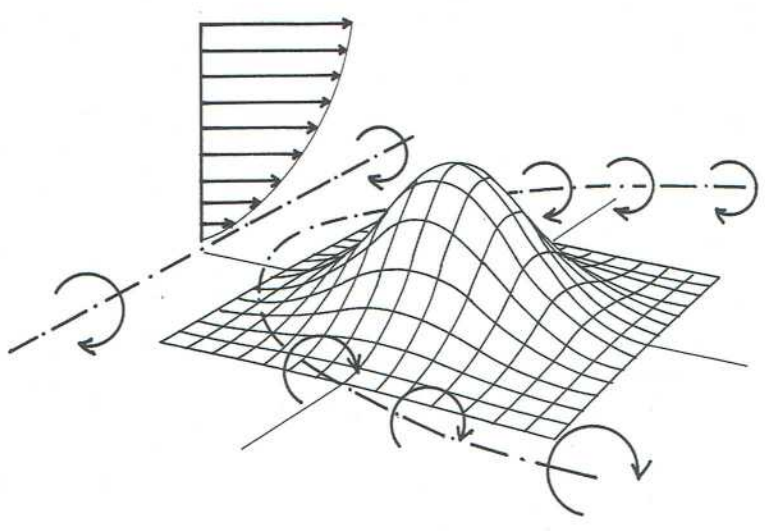

Fig. 4.3:
Horse shoe vortex. See text.

Fig. 4.4: *Dividing streamline concept.*
Flow from left.
Flow up to height H_c nearly in horizontal plains around the obstacle (regions I, III).
Flow above H_c = 3-D gravity wave flow over "cutoff hill" (region II).
Wake flow (region IV). See text.

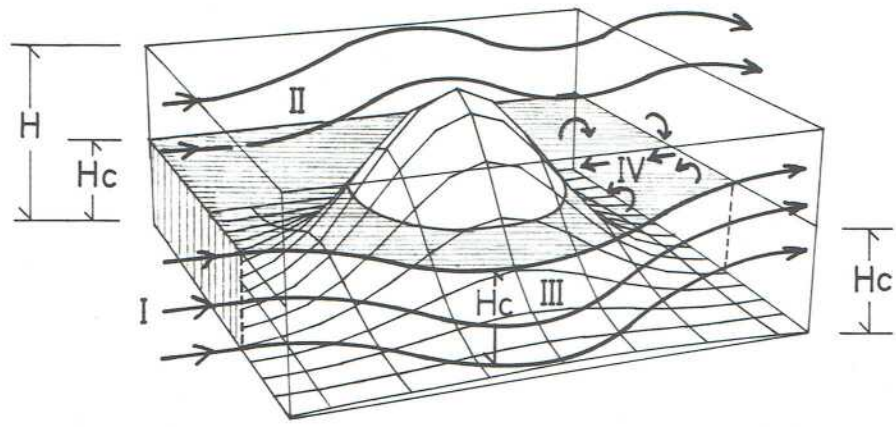

Basically, a brisk wind driving a not too stable airmass will easily be able to climb a hill not too high (F > 1), such that H_C = 0. In this limiting case, there will be three-dimensional gravity wave flow over and around the entire hill as described best by R. B. Smith (1989, or see Fig. 4.5 a).

More generally, however, the wind will be too weak, and/or the stratification too strong, and/or the hill too high, such that F < 1, and H_C < H exists (Fig. 4.4). All the air below H_C is supposed to flow in a "Drazin-type" pattern resembling potential flow in horizontal planes, with little vertical motion (region I). This air stream flows completely around the hill on both sides (only front side shown), being unable to climb it. Very plausibly, the stronger the stability, or, generally, the smaller F, the deeper will be this lower layer. Moving from the windward side to the lee, however, only the outer portions of region I stay orderly and horizontal (region III, separated flow, see Fig. 4.5 b), the inner portions eventually becoming part of the turbulent wake region IV, which comprises the entire "shadow" region of the hill up to the hill summit, extending very far downstream. Region II is above height H_C, fore and aft (but significantly pierced by the upper part of the wake!), representing the 3-D gravity wave flow over the cutoff hill.

Fig. 4.5:
Numerically computed 3-D flow around a smooth, circular obstacle (Schaer and Durran, 1994, in press).
No surface friction. U = const. (from left), N = const.
Side view and top view (surface flow).
a) Left half: Froude number F = 1
b) Right half: Froude number F = 0.33

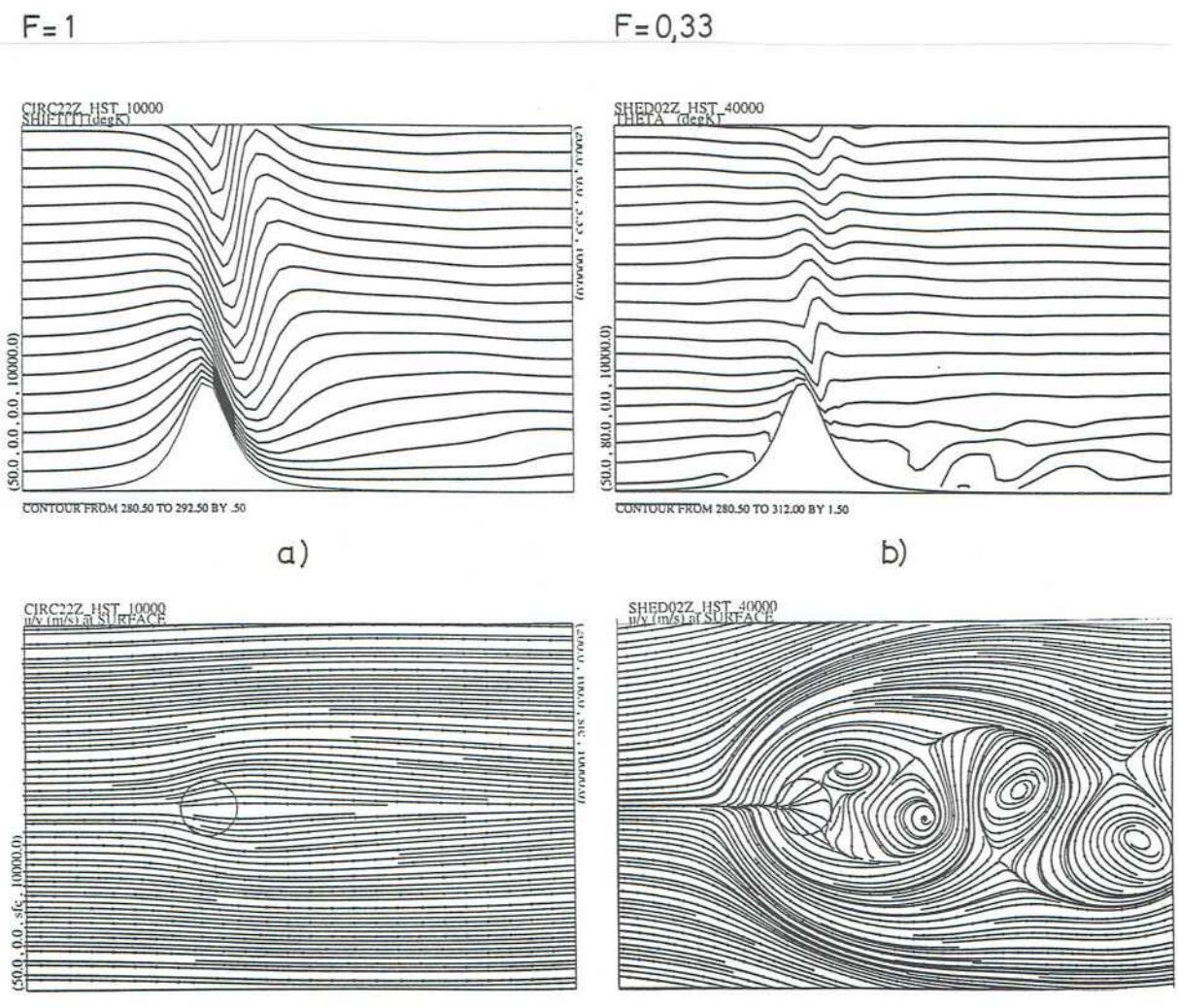

This schematic model, beset as it is by apparent theoretical contradictions and practical problems of how to determine representative parameters, still is the best attempt to bring some order into the chaos, as long as it is not mistakenly taken for a firm prescription. Consider only the fact that in the presence of two or more hills there does not appear to be a consistent way of defining H_c. The variety of flows and complications must not be forgotten!

For example, Schaer and Durran's simulation (Fig. 4.5 b) has the wake broadening to become much wider than any effective hill diameter, but such numerical results may just be too idealized and restricted in scope to fit in completely with real atmospheric variability. The authors claim that the addition of surface friction to their model runs would not have changed the results a lot. Note that Figs. 4.5 conform rather well to the criterion equ. 4.1:

For F = 1 (Fig. 4.5 a) all the fluid goes over the hill ($H_C = 0$)

For F = 1/3 (Fig. 4.5 b) $Hc \approx \frac{2}{3}H$ is not a bad guess, although some ambiguity remains. In fact, a simulation with F = 2/3 reportedly produced a very similar result, only taking more time. This would highlight rather extreme sensitivity of the flow pattern in the transition from F = 1 to slightly below 1.

The wake will contain reversed flow due to major vortices with vertical axis (Fig. 4.5 b), but certainly vortices with horizontal axis, too, unless the hill were completely devoid of irregularities like ramps. In addition, "horseshoe" vortices are a prominent feature of most wakes, being generated by an oncoming airstream with vertical wind shear (see Fig. 4.3). This vortex line, approximately maintaining its circulation, is being wrapped around the hill as shown and stretched, establishing a sinking motion in the lee. Typical numerical simulations with U = constant would, therefore, not show this vortex.

Regarding the far extent of the wake, we may perhaps imagine that the minimal turbulence due to the strong stratification is not capable of reattaching the separated flow, unlike strong turbulence would. We might suspect, therefore, that wakes on the afternoon of March 28 (Fig. 4.1, left side) would have been much smaller in extent than in conditions of more uniform stability (Fig. 4.1, right).

Once more, the remarkable result is stated that the dividing streamline concept is NOT sensitive to the horizontal extent or shape of the hill, as reflected in the expressions for Froude number F and H_C (equ. 4.1), which only contain the hill's maximum height H. This lack of sensitivity is reminiscent of hydraulic theory.

Meroney (1990) quotes Castro et al. (1983) who quote Scorer (1978) with his warning: "There is almost no systematic way of discussing the flow behind a three-dimensional obstacle of arbitrary shape when separation occurs." This warning could only be reinforced here, for

example when "surface heating further complicates the already confusing flow picture" (Meroney, 1990). For this very reason I have chosen not to discuss thermally driven circulations at all in this chapter, hoping that ad hoc meteorological reasoning and experience will suffice, when needed. For example, up-valley and down-valley ("downslope") wind regimes (see Vergeiner & Dreiseitl, 1987) should be established on a pretty day like March 28, but they might not be clearly seen as such (as opposed to the deeply cut in major Alpine valleys), probably being swamped by the prevailing southerly wind. The numerical model (chapter 3) should help us to locate any such influence.

The dividing streamline model will not be useful any more when the obstacle height H becomes small, if only because real landscapes don't look like little isolated humps mounted on flat plates. Cool air collects in low-lying places, and rather low hedges or other structures will suffice to dam up that cold-air pool, even if it may periodically spill over. In another situation, a row of buildings may well be responsible for preventing fresh, cool air out of a ravine from ventilating part of a city. It was mentioned at the end of chapter 2 that well-protected patches of cold air over low-lying terrain must have resisted the advances of warm air on March 29 and on March 30. These patches would tend to be less harmed by TMI-contaminated plumes or puffs. Being extremely stable, however, the affected air column might distort the air flow in ways which would make detailed analyses of transport and dispersion hopeless beyond the reservations expressed throughout this chapter.

Wakes behind obstacles like the one shown in Fig. 4.5 b are not stationary, but unstable to small, ever-present perturbations. In real nature, they collapse and move downstream, while new wakes are being formed. This is true even in most laboratory and numerical experiments, where the oncoming flow is kept stationary: The Kármán vortex street with its periodic shedding of eddies is the best-known example. Separation of wakes should be enhanced when the oncoming flow is changeable, as in real nature. It is impossible, however, to quantify this very sensitive process.

Wakes behind buildings (= cavities) will not be treated here. This is a science in itself, or rather more an art than a science. Reference is made to the "Atmospheric Dispersion Estimates for TMI Unit-2 Vicinity of Plant Structures" by J. Halitsky, which should be read with amusement and some appreciation of wizardry, but also with some legitimate questions in mind: How sensitive would his results be to certain fairly arbitrary assumptions, to the inclusion of omitted

atmospheric structures, to wind directions other than 157.5°? Shouldn't such keen hypotheses be tested in a wind tunnel?

In any case, the issue of which fraction of a puff or plume gets entrained in various cavities is of some importance for interpreting release szenarios. It seems doubtful that this enormously complicated flow problem has reproduceable answers, so we must consider each regime as being within the range of possibilities. For mere visualization, it may still be useful for the reader to "downscale" some of the observations on wakes and respective figures presented here, including the issue of wake collapse and re-formation, although the studies were not done for building cavities.

The inferences of all this for the fate of TMI releases will be pursued in chapters 5 and 7. Clearly, no more than exemplary pictures of possible or plausible scenarios can be expected. Actual trajectories of air parcels or puffs can be extremely complicated, including reverse flow down the windward slope. Partial upstream blocking may occur. As an upshot of Figs. 4.4 and 4.5, one of the most relevant flow features must be the "stagnation streamlines" leading up to the windward stagnation points in the lower layer. When these or neighbouring streamlines carry radioactive plumes, the latter may get near to the hill slope in undiluted high concentrations, a process well known and documented as "impaction".

5. Transport and dispersion on the local scale

5.1 A brief status report on short-range dispersion models, Gaussian and beyond.

Distances on the order of 10 km or 10 mi, roughly, are understood when using the term "short-range". The term, however, implies much more:

a) A quasi-stationary meteorological situation, that is:
Wind direction and speed, height of boundary layer, intensity of turbulence and the like.
all staying roughly constant for at least, say, one hour

b) All these relevant meteorological fields are taken as homogeneous in the horizontal, i. e. for example the wind field is assumed to be uniform everywhere, varying at most in the vertical direction. Winds and stability measured on-site are taken to be the same out to, say, 10 km!

c) Flat terrain, or, at most, gently rolling countryside is either explicitely or tacitly assumed.

d) As a rule, models and concepts are based on continuous and constant rates of emission of gases and particles, including, of course, parameters governing the "effective" height of emission like exit velocity, excess temperature and liquid water content.

We note in passing that the Defendants have made use of a particular, namely Gaussian short-range transport and dispersion model. Without foreclosing a more detailed exposition of that in sub-chapter 5.4, two points are made right away:

- The Defendants = P & G = Woodard have so far not bothered to take note of any of the topics treated here in chapters 2, 3 and 4, obviously assuming that they don't need to.

- The Defendants, recognizing the severity of the restrictions a) through d) in a practical application, are relaxing the limitations in various ways, most obviously by using new parameters every 1/4 hour. Homogeneity, however, remains rigidly imposed. The least we would expect in this case would be that they, rather than insist on three-digit accuracy, acknowledge the very questionable and empirical nature of these ad-hoc modifications.

The classical Gaussian dispersion model is still being widely used in regulatory practice, although the conditions for its tolerable validity are often violated and its principal shortcomings have been realized for some time. At its core is a mathematical expression for the concentration field C (Ci/m^3), when the wind u (m/s) carries off a continuous release Q (Ci/s) from a stack with "effective" emission height H_e to form a plume, much like the one shown in Fig. 1.1:

$$C = \frac{Q}{2\pi \cdot \sigma_y \cdot \sigma_z \cdot u} e^{-\frac{y^2}{2\cdot\sigma_y^2}} \cdot \left[e^{-\frac{(z-H_e)^2}{2\sigma_z^2}} + e^{-\frac{(z+H_e)^2}{2\sigma_z^2}} \right] \qquad 5.1$$

Here x is distance downwind from the stack, along the plume axis
y is distance across the axis,
z is vertical coordinate (ground = flat plain: z = 0),
and σ_y (x), σ_z (x) are empirical "sigmas", being Gaussian standard deviations of the plume in the crosswind and vertical directions.

The plume axis = line of maximum concentration is assumed to be a straight line down-stream from the "effective height of emission" z = H_e, which may exceed the stack building height considerably.

For this expression to even theoretically hold true, the wind would have to blow "long enough" from the same direction, all other conditions also being unchanged. Very significantly, if the wind u drops to zero, concentration C increases to infinity! This breakdown is a signal that equ. (5.1) relies on an infinite mixing volume such that the concentrations C everywhere do NOT increase with time despite continuous emission! Equ. (5.1) might be called an elegant cover-up of the mass balance:
Where do the curies actually go?
Equ. (5.1) is, therefore, no good for calms or near calms, but it should be added that the Gaussian model can be operated in a "puff mode", i. e. simulating a sequence of short "bursts" of emitted material. In this "puff mode", the above fallacy is avoided.

The sigmas are highly empirical indications for the width of the plume, given for "stability classes" A (very unstable), B, C, D (neutral), E, F through G (extremely stable). The most popular scheme is Pasquill & Gifford = Turner (1970), but many other sigmas have been proposed and used.

Equ. (5.1) as it stands assumes unimpeded upward dispersion - in many cases a very wrong assumption. There is, however, a useful approximation accounting for "reflections" from the underside of an inversion layer, analogous to the sum of two terms in brackets, expressing reflection of the material from the ground surface (see Turner, 1970). Thereby, the finiteness of the "mixing layer" will be taken into account.

Although equ. (5.1) is a fairly boring exercise, expressing no more than the fact that the "flux" of released substance through any cross section perpendicular to the plume axis, whether the plume be wide or narrow, must equal the rate of emission Q, the inferences are not trivial. To take just one example: According to the old schemes for computing "plume rise" due to excess momentum and buoyancy of the released air, the plume would almost freely penetrate elevated inversions. In this way, "effective" stack height H_e might easily be, say, 150 m instead of the building height of 50 m, bringing down maximum ground level concentrations by a factor of $\approx \left(\frac{50}{150}\right)^2 \approx 1/10$, unless surface concentrations were outright set to zero.

In addition, dry and wet deposition of emitted gases and particles onto natural or artificial surfaces should be taken into account, a very complicated series of processes which also serves to remind us of the likelihood of physical and chemical transformations acting on the releases. In bypassing these issues to a first approximation, I definitely do NOT intend to set a precedent. I simply submit to some necessary limitations. Deposition would have to be very efficient to noticeably deplete plume or puff concentrations along the first five or ten miles.

The growing dissatisfaction with the Gaussian models was expressed in a peer review of verification attempts for 10 regulatory diffusion models (Smith, 1984). Numerous proposals for improvement were made (Irwin & Smith, 1984, Weil, 1985), addressing some of the major criticized points:

- Pasquill - Gifford dispersion curves are derived for ground-level releases only.

- P & G stability classes have an extremely strong bias towards neutral stability, whereas either stable or unstable conditions are much more frequent.

- Plume penetration of elevated inversions is "all or none".

- Systems to correct for terrain height (by the way, precisely as recommended in NRC Regulatory Guide 1.111 and apparently applied by Woodard) are considered "crude and scientifically unproven".

- Severe underpredictions were prevalent in stable conditions.

- Model evaluations on several data bases turned out to be quite disappointing, even for level terrain.

- Very high sensitivity of model predictions was noted to even slight errors (only two degrees!) in estimating the transport direction.

- Winds measured at a particular height, even if perfectly accurate, would not be fit to define actual transport direction at plume elevation. This consideration applies a fortiori to our extremely stable case with the wind direction shifting markedly with height.

- Mixing height, recognized to be an essential ingredient in any diffusion model, is well defined only in ideal conditions, being very ambiguous in most cases (Hanna, 1992). Quote: "Which little blip (in the radiosonde profile) represents the mixing depth?"

It would be fair to state that a new generation of boundary layer models including dispersion has emerged in the course of the last ten years. Only some of their features will be highlighted briefly. The pertinent literature is enormous, and this cannot be a literature review. Some judgement is necessary, in line with Islitzer and Slade's statement (Slade, 1968, p. 173): "The meteorologist must in more complicated terrain use his total experience to assess, even qualitatively, the nature of the resulting diffusion." And ibid., on p. 188, where the same authors point out the relatively ideal conditions chosen for diffusion experiments, as opposed to the adjustments necessary in real-world conditions:

"... these procedures contain elements of both science and art, and here the inflexible guides of a handbook must yield to the acumen and imagination of a trained meteorologist."

Fig. 5.1:
5.1 a to c: *Non-buoyant plumes (from Stull, 1989)*
a) elevated release
b) ground release
Horizontal axis: Nondimensional downwind distance
Vertical axis: Nondimensional height (1 = top of mixing layer)
5.1 c: *Idealized snap shot of plume, illustrating vertical meandering.*
5.1 d: *Buoyant plume (from Willis and Deardorff, 1987)*
Smoothed contours of the crosswind-integrated dimensionless concentration $\overline{C}$.

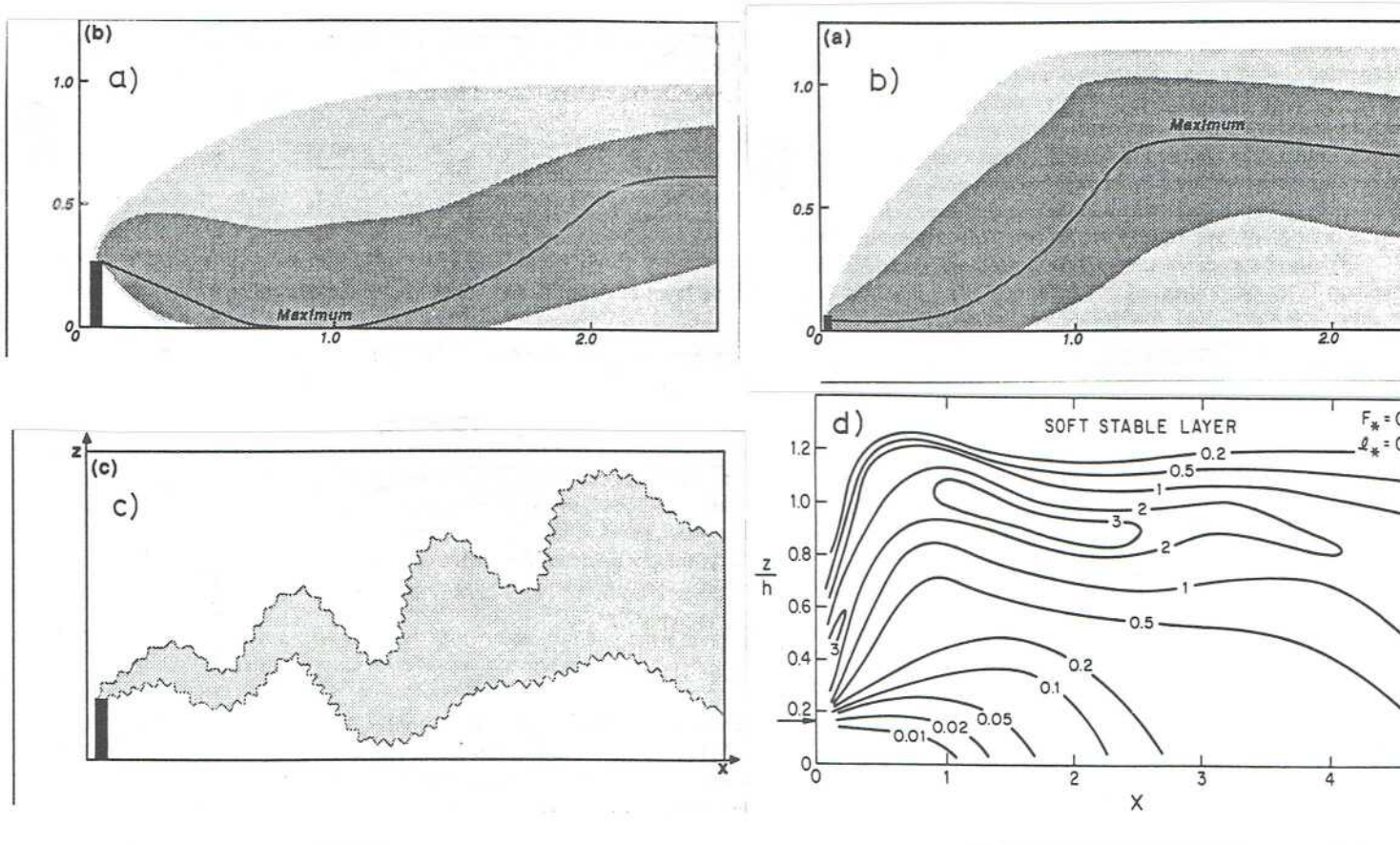

Typical features of these new models, e. g. HPDM (US Hybrid Plume Dispersion Model) or OML (Danish), are:

- More complicated "sigmas", being functions of travel time $t = x/u$ rather than downwind distance x, and continuous functions of convective scaling variables

- Complicated radiation balance, heat balance and hydrological schemes

- Comparatively realistic description of the daytime unstable "convective boundary layer" = CBL under clear skies, mostly following the work of Willis and Deardorff (1978, 1987, Deardorff and Willis, 1975, and others).

These new results show some features clearly at odds with Gaussian theory (see Fig. 5.1), which has maximum concentration along a horizontal axis:

Non-buoyant plumes are eventually carried upward, before being dispersed uniformly with height between the ground and the top of the mixing layer (Fig. 5.1 b). In case of an elevated release (Fig. 5.1 a), the plume first descends to the surface!

Buoyant plumes have an entirely different "signature" (Fig. 5.1 d):
They quickly rise to the top of the mixed layer ("lofting"), even partially penetrating the overlying inversion layer. Significant concentrations of the effluent near the surface do not appear until further downstream, and the vertically well-mixed state ($\overline{C} = 1$ in this terminology) is attained only at distances $X > 5$, which may correspond to more than 20 or 30 kilometers. By the way, the concept of final plume rise loses much of its relevance in the light of the above findings (see also Scorer's critique of that concept as early as 1958, 1st edition, 1978, 2nd edition).

These features may be explained in terms of the dynamics of organized, long-lived thermal plumes in the CBL (pdf-theory).
Releases on the late morning and afternoon of March 28 would possibly fit into these concepts (see Figs. 2.2 and 4.1), but some problems remain:

- The CBL-theory is only for flat terrain, and

- It applies to continuous releases = "plumes".

If the releases are more like instantaneous "puffs", modifications are not straightforward.

- Inherent uncertainty and variability is due to vertical (Fig. 5.1 c) and lateral plume meandering. Large mesoscale eddies responsible for these concentration fluctuations will depend on the actual site-specific flow pattern. Weakly buoyant plumes will show more highly fluctuating axes, as opposed to the strongly buoyant "lofting" behavior. Fig. 5.1 c is a good illustration how large, longer-period eddies transport the entire puff, whereas small-scale, short-period turbulence tears it apart, thereby diluting it.

HPDM and similar models are presumed to be applicable in neutral and stable conditions, too, and, with empirical modifications, for gently rolling terrain. Problems are mounting rapidly, however. Generalizing a quote from Hanna & Strimaitis (1990, p. 114): The highest class of regulatory model to be applied to rugged terrain and stable stratification, the "refined model", is an empty set at the moment .... CTDM ("Complex Terrain Dispersion Model") and related British (ADMS) and US model developments, based on concepts like the "dividing streamline height" (see chapter 4), are in an experimental stage.

I will argue further down that the extremely interesting new concepts should be applied on an ad-hoc basis, combined with critical judgement of factors specific to the site and to a particular weather pattern. An automated, routine description of the stable boundary layer in rugged terrain is, however, clearly far beyond anyone's capability. In this respect, HPDM- and similar parameterizations are essentially useless, much as they may reflect ingenious collections of available knowledge and voluminous research. This seemingly harsh judgement is borne out by model tests and evaluations (Hanna & Paine, 1989, Hanna & Chang, 1993): Even when emphasizing convective and neutral conditions, working in nearly flat terrain and not using completely independent data bases for evaluation, model performance remains disappointing. Correlation coefficients between observed and predicted concentrations "paired in space and time" are often negative. When the locations of observed and predicted maxima are permitted to be different, still only 20 % would typically be within a factor of two of the true value, and only longer-term averaged maxima might show unbiased model performance.

In any practical application, a typical problem arises, as a number of parameters needed for the more involved boundary layer parameterizations (like the Lagrangian time scale) are not measured or

not derivable from the available external data. They must be chosen in the "default" mode or in some other arbitrary way, with possibly unforeseen consequences.

5.2 More on the mixed layer

In the following, the rather abstract term "mesoscale eddies" will be given some life. Regarding notation, "convective boundary layer" tends to imply weak wind, whereas "mixed layer" is preferred for cases where horizontal advection must not be neglected. "Plumes" will, for the moment, be bubbles of warmer air from the surface layer, rising and travelling with a mean wind speed, and merging to form "thermals" with diameters on the order of 1 km, extending throughout the mixed layer. However, favourite "hot spots" on the ground will form stationary plumes, which may eventually be ripped off like separating wakes. Updraft velocities within the thermals are typically 1 - 2 m/s, downdraft velocities a bit less, but covering a larger area. An air parcel or puff circulating within the CBL will remain either in an updraft or downdraft typically for 5 to 15 minutes.

Stronger winds tend to disrupt thermal convection, but they help to establish organized helical circulations over undisturbed level surfaces: pairs of clockwise and counterclockwise rotating roll vortices with axes along the wind direction (Stull, p. 468).

By no means should the impression prevail that motions in the CBL are all regular and orderly. Irwin & Smith (1984) report on an entirely unexpected case, when apparently a puff was brought down to the ground from a tall stack during extremely unstable conditions, moving slowly about thereafter and diffusing its high effluent concentrations only very gradually, as opposed to the highly efficient dilution predicted by Gaussian theory.

One of the most significant features within both the unstable and the stable boundary layers are internal boundary layers. Let the wind blow over smooth grassland with enough "fetch" to establish the proper boundary layer in equilibrium. Let the wind then cross over to a forested area (Fig. 5.2). A new boundary layer will form over the rougher surface, growing slowly downwind as indicated in the very schematic figure, whereas the "old" boundary layer above will not feel the "new" surface. This pattern may be repeated as shown, such that very complicated layering may result even over flat terrain.

Fig. 5.2:
Internal boundary layers within internal boundary layers, typical of flow over patchwork land-use patterns (from Stull, 1989).

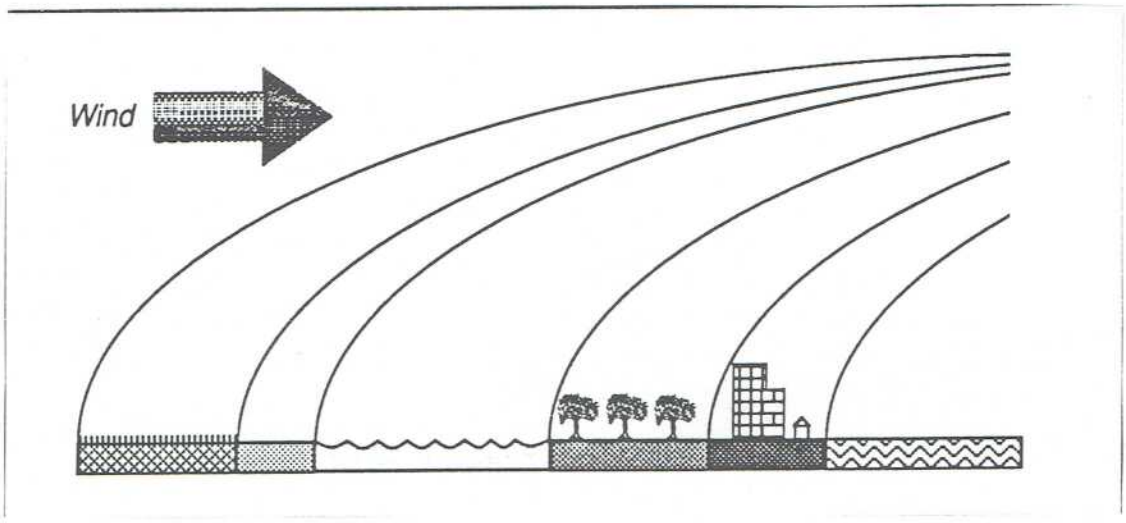

Fig. 5.3:
Layers within the urban boundary layer (from Stull, 1989).

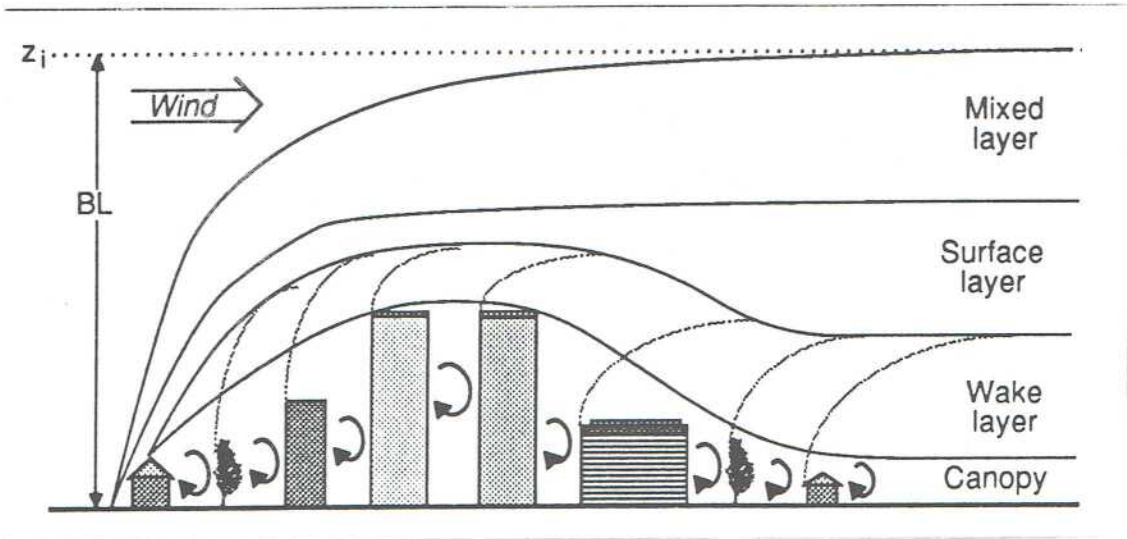

Now let, for example, the wind blow from across the Susquehanna River towards TMI Island. The river would be cooler and, of course, smoother than the land, with the reactor building complex being warmer and rougher yet. New "thermal internal boundary layers" will form due to the different heat fluxes at the underlying surfaces, in addition to the frictionally controlled internal boundary layers, and the two will, in general, have different vertical depths. All this can happen in stable and unstable conditions, the difference being that surface forcing penetrates upward more readily and more deeply in unstable conditions.

Fig. 5.3 gives a taste of the possible resulting structures, with a city as a source of large thermal and frictional anomalies. We may imagine the TMI reactor and cooling tower building complex as a mini-city with urban plumes emanating from it, and wonder how representative winds or temperature gradients might be, measured on a meteorological tower either downwind of that complex or downwind of the river and hills.

5.3 The stable boundary layer - transport and diffusion

Referring to the synoptic situation (chapter 2), the boundary layer had to be stable or extremely stable most of the time. This case is, therefore, of paramount importance.

The stable boundary layer (SBL) is very different from the unstable CBL discussed above (see Hunt, 1985, Weil, 1985). It contains only weak and small-scale turbulent intensity; there is no steady input of thermal energy to feed vertical displacements. Therefore, the variance of vertical velocity fluctuations $\sigma_w^2 = \overline{w'^2}$ is small. A limiting expression for vertical plume thickness = σ_w/N reflects the suppression of vertical motions by stable (negative) buoyancy forces (for N see subchapter 2.3). Vertical plume dimensions on the order of 10 m or smaller have been demonstrated, presumably under conditions when the release's own (positive) buoyancy made little contribution to form a well-mixed region of sufficient scale initially.

Paradoxically, the weak level of turbulence in the SBL activates another driving mechanism for turbulence: Due to the weak coupling of adjacent layers, large "wind shears" = changes of the wind direction and speed with height will typically occur in the SBL (see e. g. Fig. 2.2.). The practical resolution of this seeming paradox appears to be that turbulent "patches" are formed within the SBL, outside of which the air may be essentially quiescent. Turbulence is said to be "intermittent" in space and time - a good example of the inherent variability and uncertainty of atmospheric processes.

A puff released from a stack, therefore, might be carried around by the air currents essentially without being diluted by the small-scale turbulence at all. It would, however, still be subject to another mode of dispersion: being displaced upward and downward a little, some elements of the puff would, due to the wind shear, be carried off in different directions at different speeds.

The problematic nature of the SBL is not limited to dispersion features. Its height, ranging from a few meters to a few hundred m, is ill-defined and parameterized even worse. It is highly instationary and inhomogeneous in the vertical and in the horizontal:
Any small changes in local topography (even slopes of 10^{-3} are quoted as having significant effects) or local weather conditions or surface conditions will affect the boundary layer for a long way downwind; signals from the surface may take hours to be felt on top of the SBL, such that equilibrium can never be established.

Internal gravity waves are a recurrent feature of the SBL, as well as drainage flows of thermal origin (Derbyshire, 1992). As Hunt remarks, you don't need complex terrain to have complex flows in the SBL. Small wonder that field experiments for testing boundary layer models take place preferably on the plains of Minnesota, in the Netherlands or in the Australian desert.

In summary, flow and turbulence are not determined by local parameters in the SBL, in strong contrast to the CBL. This highlights once more the inherent natural variability and unpredictability of the local SBL properties, on top of the large model uncertainty. A last pertinent key-word is "meandering": Plume meandering is not specific to the SBL: In fact, vertical meandering is restricted to the CBL (see Fig. 5.1 c) and is an important reason for concentration fluctuations, as wisps of a plume embedded in the fairly large-size up- or downdrafts tend to stay there fairly long.

Lateral meandering, however, is particularly conspicuous in stable conditions, when a fixed monitoring station is alternately exposed to the undiluted plume, or stays completely outside of it. Averaging concentrations at the site, some low value may result if a very narrow plume hits the site only rarely. But this is not the whole truth: Let the undiluted plume impact on a hill slope (see chapter 4) and let a part of it be caught to stagnate in a suitable concave place (see chapter 7). Then very high concentrations of, say, radioactive gases or particles may act out their disastrous effects over a sufficiently long time.

The low-level jet (LLJ) is a recurrent feature of nighttime stable boundary layers (see Stull, 1988). Nighttime down-valley winds reaching out into the plains peak at 10 - 20 m/s between 100 and 300 m a.g. in the early morning hours, when friction diminishes due to decoupling of adjacent stable atmospheric layers. There are many quite different types of LLJ, but they are not pursued here in detail, as it is not expected that they play a major role in our investigation.

This brief discussion will serve to validate my previous conclusion that ad-hoc use of the various concepts is the most reasonable thing that can be done, taking account of both the state-of-the-art in flow and dispersion modelling, and the uncertainty inherent in a particular realization of CBL or SBL behavior.

5.4 A preliminary critique of K. Woodard's Gaussian meteorological model and his methodology.

This piece is being written before we have had a chance to learn more about Woodard's proceedings and to understand in detail how he arrived at his results. Therefore, conclusions are based on his written Exhibits only, and on comparisons with my own work.

I will not repeat here the very fundamental reservations against the Defendants' presentations and claims, as expressed and argued in chapter1. Also, we cannot spare Woodard the reproach of not having bothered to present a single piece of evidence on the general synoptic weather situation (chapter 2), regional flows (chapter 3), local flows (chapter 4) and advanced boundary layer and diffusion models (subchapter 5.1, 5.2, 5.3). This failure is all the more disturbing as even the NRC Regulatory Guide 1.111 spells repeated warnings to take account of regional meteorology and regional airflow. The reader must draw his own conclusions as to how much a model could be worth which reduces the contents of these chapters to a wind and a temperature difference measured on the meteorological tower. And to make bad things worse: By all standards, the representativeness of these point measurements could only be very poor (see chapters 4 and 5.2).

The status report on short-range transport and dispersion models (chapter 5.1) together with more recent results on boundary layers (5.2, 5.3) should have made it evident that the Gaussian model used by Woodard is substantially out of date, notwithstanding its empirical ad-hoc modifications. Again, the listing of the most relevant items will not be repeated.

The tower data could not be representative even of the near vicinity of TMI with its very complicated river and hilly topography. Consider, for example, the substantial, even extreme variability of measured winds at Harrisburg, Middletown and TMI, plotted for easy comparison in Fig. 2.3. And wind measurements at airports are more representative than at many other sites.

Consider, furthermore, numerically computed regional wind fields as shown in chapters 3 and 6. The wind field and thermal stability simply couldn't be homogeneous, not on the local scale and even less so on the regional scale. Woodard has it that his point measurements are valid out to a distance of 50 miles!
Consider, last not least, the szenario of plumes or puffs impacting on hill slopes (chapter 4). Woodard might claim that the NRC-approved technique of correcting the "effective release height" for terrain height makes due allowance for impaction. It will be demonstrated, however, in chapter 7 that this "crude and scientifically unproven" method keeps us far away from reality, unless realistic flows and realistic dispersion are admitted.

A basic flaw of Woodard's model is its neglect of mixing height, leading to systematic underpredictions.

In short, Woodard's model is "out" definitely by orders of magnitude, when it claims to predict concentrations (MPC's = annual average concentrations) or radiation doses (mrems) beyond the immediate vicinity of TMI, even to discriminate between populated places and others with "no permanent residents". There is no scientific basis for such a claim. The situation in the immediate vicinity of TMI needs to be examined separately, however. This is because Woodard calibrates his assumed releases on the TLD readings, using his model as a "transmission link".

Starting with some general remarks, Woodard's recent segmented plume model is definitely an improvement over earlier versions, even if he appears to say that his results never get changed. It must be clarified, however, whether the azimuthal and radial resolution used was much too coarse (see chapter 7). The "variable trajectory" mode implicit in this recent model is, unfortunately, spoiled by the fact that winds and thermal stability at distance are definitely not the same as on the tower. In fact, measured values on the tower are most likely not valid for the actual point and height of release: The meteorological tower and

the vent stack are some 200 m apart, and located in different regions of various building or building complex cavities (Halitsky, 1979).

Given the sobering experience in trying to peer-review and verify dispersion models better than the Gaussian models (chapter 5.1), and given the obvious inadequacy of wind and stability input to the model, the present Gaussian model definitely cannot predict the location and strength of near-surface effluent concentration maxima in individual hours, or for individual release "events". This capability would be contrary to all evidence. This issue raises the legitimate question whether the NRC models have ever been verified in well-controlled conditions regarding releases, transport and dispersion conditions and radiation measurement network.

If the model were physically free of major faults (which it is certainly not), it might give fair predictions in a statistical sense (e.g. ensemble of a year's hourly values), but not for individual hours. Thus, any good short-term correlation between measured and predicted concentrations would have to be fortuitous - or falsified. However, we have to be careful extending this line of reasoning from concentrations to γ-dose measurements or computations. Woodard correctly states that γ-dose is less sensitive to plume shape or location and other uncertainties than effluent concentration. After all. looking at Fig. 1.2, there will be a γ-"signature" on the ground even when the effluent concentration there were zero. A γ-dose measurement amounts to some kind of integration over space, and, of course, over time. Still, there is sensitivity as shown in chapter 1.6 (Fig. 1.2), which would apply to a very stable, narrow plume. Regarding the daytime unstable situation with an eye on Webb's blowout during the afternoon of March 28, I have estimated γ-doses (soft γ) as seen by a TLD for two assumed plumes, hitting the TLD straight-on, exactly along the lines and assumptions laid out in chapter 1.6, equs. 1.1 and 1.2, with suitably adapted geometry:

1. Width = 100 m, height = 50 m Result: D_{γ} = 350 mR/hour

2. Width = 400 m, height = 200 m Result: D_{γ} = 30 mR/hour.

Compare this with the elevated plume in chapter 1.6 (directly overhead):

D_{γ} = 100 mR/hour
(All values for Xe-133 only)

Considering the very substantial uncertainties of plume size, shape and travel direction alone (containment cavity, building cavity, low-level inflow of cooler air from the river towards the warm building complex, plume meandering in the boundary layer), three-digit accuracy or better would seem offensive. I do conclude, however, that if the Webb blowout is a valid estimate, near-site TLD readings should have been appreciably higher in the N or NNW direction. This is because of all the additional nuclides, some with very hard gammas. Another consequence is that radiation doses (β and γ) to company employees staying outdoors on the site for any length of time would have been frightening. By the way, a ground measurement of 210 mR/hour is noted between 4 and 6 p.m., March 28, in the Defendants' Sequence of Events. Helicopter-based measurements are quoted with over 1000 mR/hour on March 30 (No measurements on March 28!). Offhand, such values at 600 ft a.g., if more than momentary events, would appear to imply either quite substantial plume rise or enormous venting releases.

Questions over questions. The status of the TLD's remains the most important one. The critique in chapter 1.6 can only be reiterated here. Anyone familiar with the snags of instruments and people would demand proper documentation of servicing, calibration and measurement procedures.

We have to wait for a fuller understanding of how Woodard's model works, how he simulates certain TLD readings. Which nuclides considered , which retention factors as a function of time, which release mechanisms and amounts? Initial plume size, rate of plume spread? How reliable are the ventilation rates? Is the excess temperature completely negligible? The question of whether particular releases were ground-based or elevated remains entirely unresolved: Not only is there a large discrepancy in the fraction, when a plume can be considered a ground release, between the values used by Woodard and the very low fractions calculated by Halitsky for the vent stack. More than that: Leaks in the ventilation exhaust system may have been more efficient pathways for gaseous radionuclides than the stack.

Which TLD orientation, which γ-sensitivity and which cutoff assumed? As for the back-tracking method: Since releases seem to have occurred in bursts, each in a characteristic wind direction, roughly speaking, with only one or two TLD's carrying the burden of the proof, it would be relatively easy to "tune" the model to the TLD's or, more bluntly, to "doctor" it if one wanted to. All the available data must be used and cross-checked against each other to try to obtain consistent pieces of the whole picture.

Regardless of what we may still learn about the releases, it bears repeating here that Woodard's model is not fit at all for predicting effluent concentrations or doses to people at any distance from TMI. In fact, no available model could predict concentrations for particular places and times with any degree of confidence (see chapter 5.1), although some state-of-the-art experimental models would be able to simulate, say, impaction on hill slopes (see chapter 7).

Last, not least, it is a mystery how Woodard and others could keep implying that γ-doses "seen" by a TLD would be actual "whole-body" doses suffered by people. And worse yet, that the highly damaging β-radiation could be all but ignored (see chapter 7).

6. Numerical Model Results
Regional Transport

6.1 Some qualifications

The model itself and a couple of computed wind fields were discussed in chapter 3. Before presenting some more results out of the total simulated period March 28 04 E.S.T. to March 29 08 E.S.T., some qualifications must be made. It would be unreasonable to expect that I could cover both local dispersion around TMI and regional transport in depth within the given time and resources. My main task was to help understand the enormous seeming discrepancy between mrems according to the Defendants and hundreds of rems according to the Plaintiffs out to, say, 10 miles from TMI (see chapter 7).

As stated before, any model can be no better than the initial and boundary values used as input, even if the model physics were perfect. The model physics is, of course, not perfect. Here is a list of some limitations:

- The model is forced by geostrophic winds at two levels, with linear interpolation in between and beyond.

- Thereby, cold- or warm-air advection is assumed to be independent of height.

- By taking vertical profiles east of the Appalachians as input, we cannot accomodate the even stronger warm-air advection on the western side.

- Open boundary conditions may introduce unwanted disturbances, although, in principle, they shouldn't.

- A frontal zone or, more precisely, the pertinent inversion can be prescribed only as initial condition on the vertical temperature profile. Its subsequent evolution must be tested against real data.

These limitations must be laid out and understood clearly. This means that a lot of checking and cross-checking must be done on any model run, before we can trust the results. There is also a difference, of course, between predicting certain types of results which are very

plausible as flow phenomena, and their precise location, timing and pattern.

I have been served very well by Dr. D. Heimann (AMBIMET), but post-processing and printout take time, and looking at all the four-dimensional fields is simply impossible, much less performing thorough checks. In the following, I will present some highlights.

6.2 Morning releases on March 28

The radioactive clouds wander around, following the weak winds first eastward, then southward, westward and northward. For the observed winds see Fig. 2.3. The computed chaotic wind fields typical of this transitional phase between cold-air advection and warm-air advection are not shown (compare, e.g. Fig. 3.3). The local plumes must be highly variable. One computed puff on the regional scale is shown in Fig. 6.1. On this scale, all effluent clouds, no matter what release time, seem to have returned to the greater environs of TMI by noon, and moved on to the Blue Mountains northeast of Harrisburg by 14 E.S.T.

The question has been raised whether early plumes could have reached Delaware and Philadelphia on the late morning of March 28. From the data and the modelled tracer fields, this seems unlikely unless the plumes had been very buoyant and risen a few hundred meters high. High surface pressure to the east would work against such an eastward transport. We can't be absolutely sure about this, however, until the possibility of a LLJ (chapter 5.3) has been ruled out. There is simply no wind data from 100 - 300 m a.g., and we would have had to start a model run much before 4 E.S.T. to give it a chance to develop a westnorthwesterly LLJ with sufficient speed. We must await more evidence and cross-checking.

6.3 Afternoon "blowout" on March 28

The presumed very large release according to R. Webb happens to coincide with southerly winds picking up to $\approx$ 5 m/s near the surface around 14 E.S.T., turning to southsoutheasterly, but maintaining speeds more or less until the early night hours (see Figs. 2.3 and 3.2). The large contaminated patches (Fig. 6.1) as well as the new releases get blown away rapidly towards the north, not necessarily following the Susquehanna River Valley only, as the mixed layer is $\approx$ 1200 m deep. We suspect that minor portions of this effluent might have been "sucked" over lower-lying terrain onto the NW Plateau of Pennsylvania in the manner of the "shallow foehn" (see chapter 2), but the model wouldn't

Fig. 6.1:
Puff released 28/04, 100 m a.g.l.
Normalized concentrations 10 m a.g. at times 06, 08, 11, 14 E.S.T.
True north 11° to the left of apparent N (see Fig. 3.1)
Violet, red: higher concentrations
Yellow, green: lower concentrations

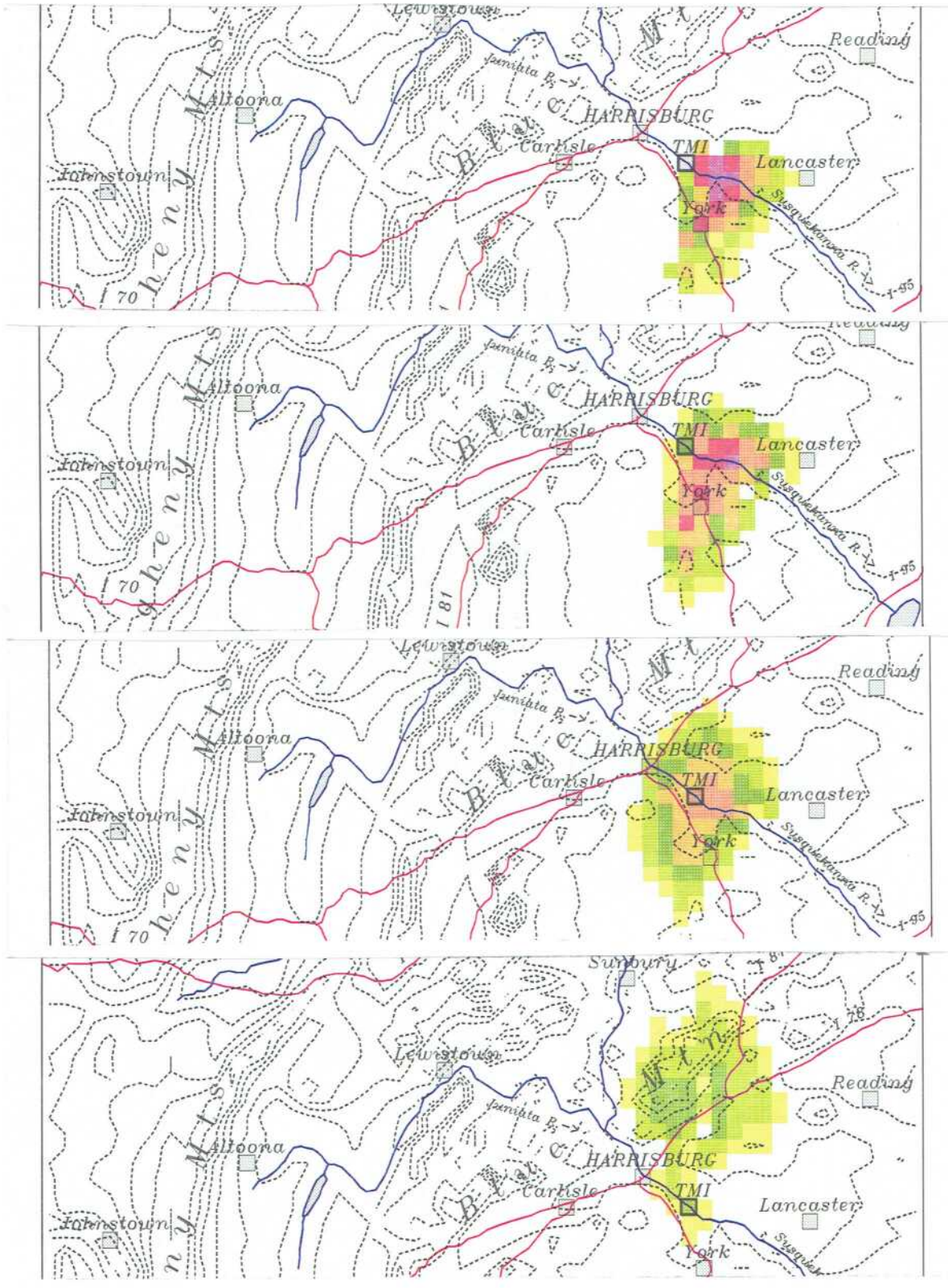

show this, being unable to accomodate the warmer air and lower pressure west of the Appalachians, as noted before.

We have printouts of the computed regional wind field on various horizontal surfaces for March 28, 14 E.S.T. Since they would take an inordinate amount of space, I show schematic vertical wind profiles only in Fig. 6.2. They should help to visualize the turning of the general wind with height, and the consequences when a plume gets raised or mixed to upper levels. The detailed fields exhibit some features to be expected, and others that are not straightforward like disturbances near the inflow boundaries and patterns of confluence and diffluence implying substantial up- and down-motions even within the inversion layer (see also Fig. 6.4).

Fig. 6.2:
Wind speeds at various levels up to 1500 m a.s.l., schematic March 28, 1979, 14 E.S.T.

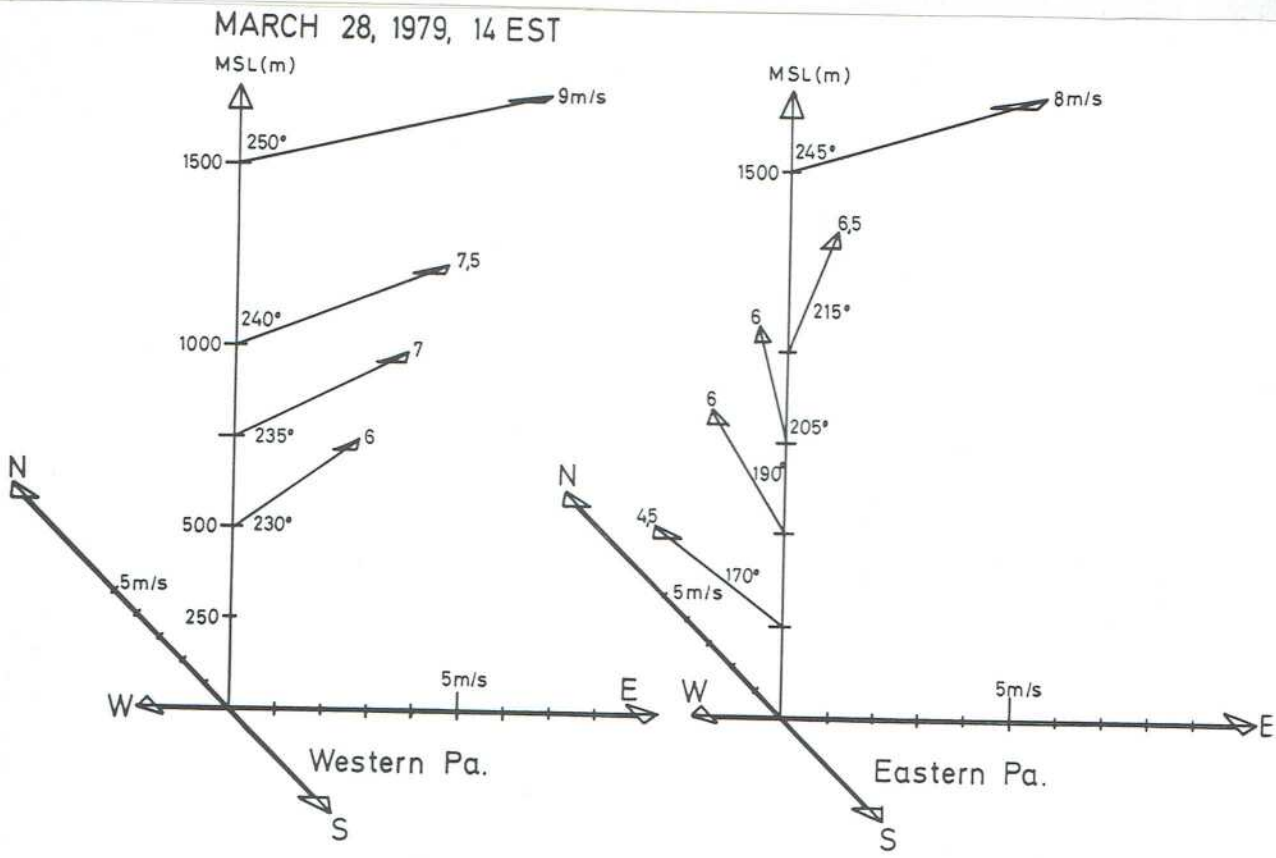

6.4 Late afternoon and evening releases on March 28

Second major plume according to Woodard
The path of these releases through the late evening and night of March 28/29 must have been subject to pronounced stagnation. This is evident from the turning of the observed winds towards lower pressure westward and dropping speeds (Fig. 2.3), well reproduced by the numerical model (Fig. 3.3 with text), and from the fact that by March 29/07 E.S.T. the frontal inversion had descended almost to the surface (see Fig. 2.2 and the discussion in chapter 2.4).

TMI plumes with release times around 14 to 17 E.S.T. get distributed across the mixing layer and travel northward. In the course of the evening the lowest layers turn cooler and very stable again. Contaminated clouds already on their way will split: The lowest parts get blocked by the various mountain ridges and become nearly stagnant. The upper parts (above the "dividing streamline height", see chapter 4) up to the former mixing height will still be carried away by the winds persisting at these levels, sometimes called "the reservoir layer". New releases are injected into a very stable atmosphere and will not reach levels much beyond their effective height of release. They will be caught in the low-level flows, partly channelled along the Susquehanna River Valley, partly turning westward into Cumberland County and stagnating there.

In Fig. 6.3 snap shots of two different puffs are shown for contrast:

Left column:	Puff released at 5 p.m., i.e. before massive stabilization
Right column:	Puff released at 8 p.m., subject to the splitting explained above.

Times shown are 1 hour, 3 hours and 5 hours after release, respectively. It is seen that the former puff moves up the Susquehanna River Valley, with ground concentrations falling off fast. The latter puff also moves upvalley, on to higher ground, with much higher ground concentrations because the affected layer is much more shallow now. Very significantly, however, a part of the effluent is blocked and kept behind by the Blue Mountains, eventually stagnating across Cumberland County west of Harrisburg.

Fig. 6.4 is a side view of the later of the two puffs shown in Fig. 6.3. Unfortunately, this is the only pertinent vertical cross section of a puff available to me at the moment, but it does show the splitting and stagnation process very well. Note that this section does not touch

Fig. 6.3:
Normalized concentrations 10 m a.g.l.
Left side: Puff released March 28, 17 E.S.T., 70 m a.g.l.
Times shown: 18, 20, 22 E.S.T.
Right side: Puff released March 28, 20 E.S.T., 70 m a.g.l.
Times shown: 21, 23, March 29, 01 E.S.T.
See also Fig. 6.1.

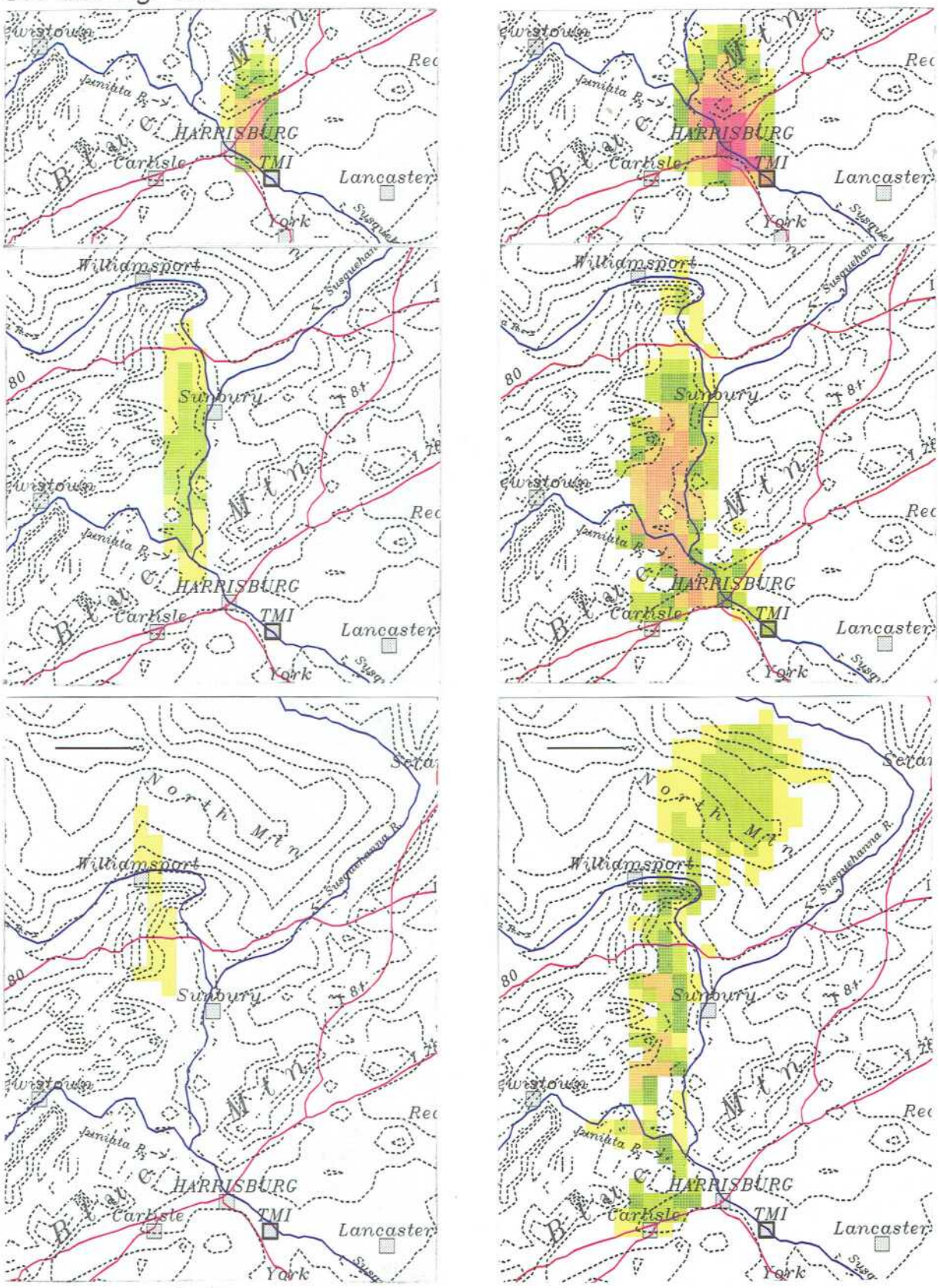

Fig. 6.4:
North-south cross section for the puff released March 28, 20 E.S.T., 70 m a.g.. The cross section runs between Harrisburg and TMI, with the Blue Mountains to the right (north).
Normalized concentrations, see Fig. 6.1.
Times shown: March 28, 21,22, 23 E.S.T.
The arrows show wind components along the cross section. They are drawn on the "sigma"-coordinate surfaces.

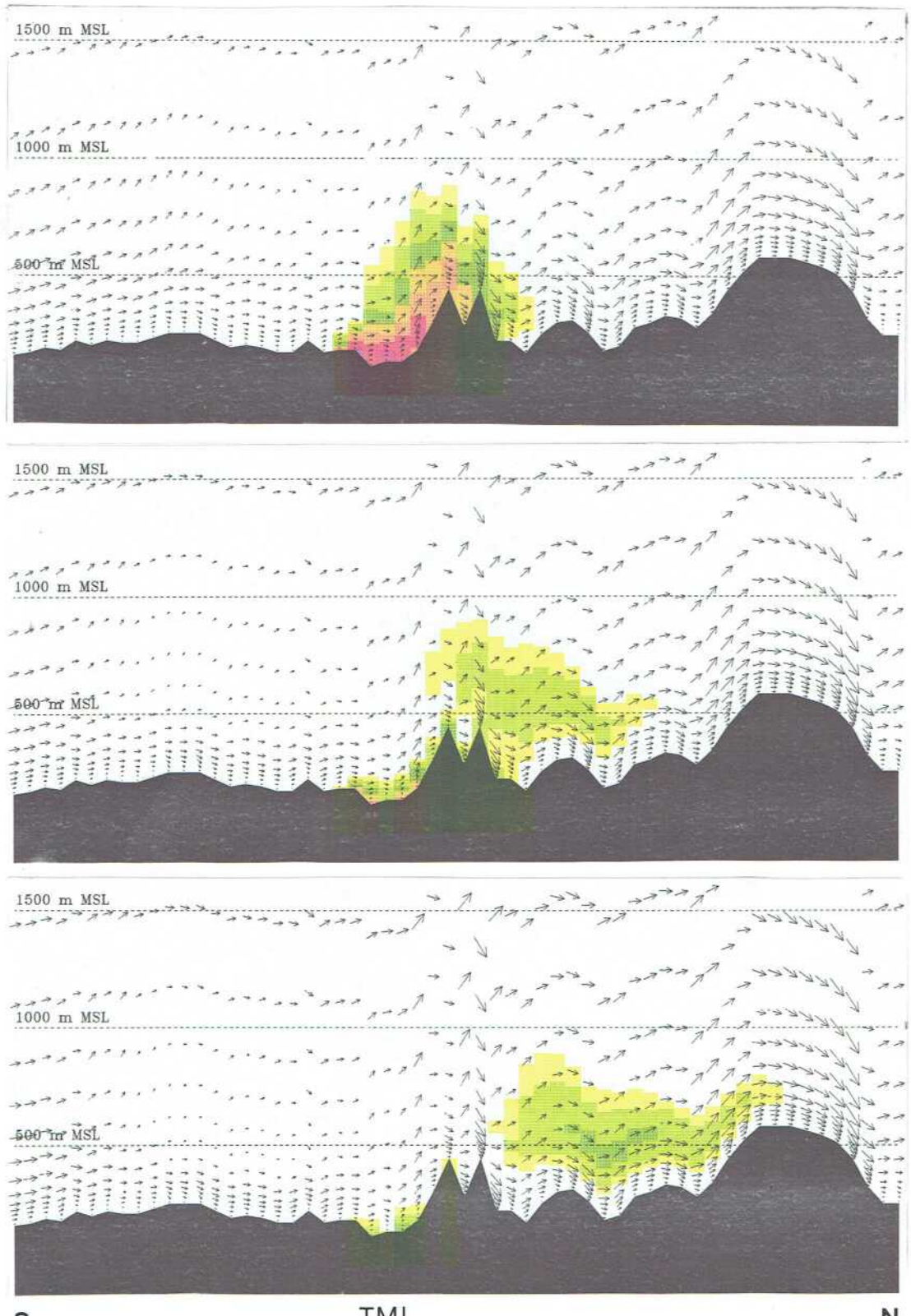

Fig. 6.5:
Puff released March 29, 02 E.S.T., 100 m a.g.
Normalized concentrations, 10 m a.g.l., see Fig. 6.1
Times shown: March 29 04, 07 E.S.T.
Lowest part: Wind field at 50 m a.g.
March 29, 07 E.S.T.
Streamline representation.

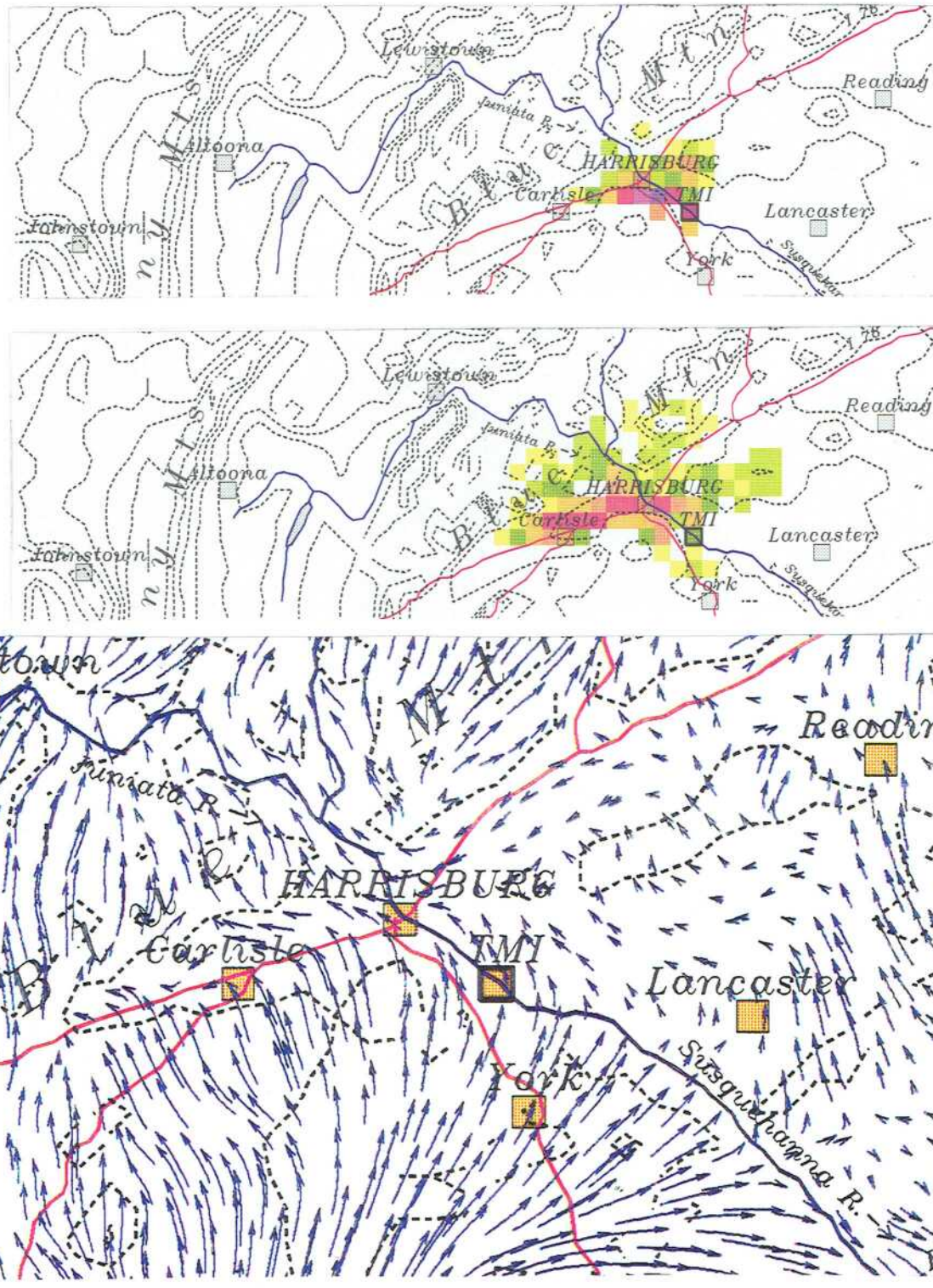

Cumberland County, but cuts through the valley and Blue Mountains northeast of Harrisburg. Stagnation is, therefore, underrepresented in this figure (compare Fig. 6.3).

Finally, Fig. 6.5 describes an early morning episode on March 29. The puff released at 2 a.m. remains relatively concentrated and doesn't travel far in the near-stagnating flow. The lowest part of the figure shows this flow once more, this time in a streamline representation. Air motions at 10 m a.g., not shown here, are very slow indeed.

This is the place to refer to the Xe-133 plume identification at Albany, N. Y. (Wahlen et al., 1980) and to the early trajectory calculations (Telegadas, 1979), tracing air parcels up from the TMI area to NY State and other Northeastern Atlantic states. From the last figures, it is obvious that, starting early afternoon March 28, TMI plumes must have travelled northward, and to the extent that they filled the mixed layer and reached the levels of southwesterly winds, northeastward (Fig. 6.2). Elevated plumes or puffs travelling in a northnortheasterly direction, partly following the eastern branch of the Susquehanna River Valley, would not show up on plots of the near-surface concentration. On their way later in the afternoon and evening, they would have cooled down, but not enough to reach the surface in this colder airmass (see Fig. 2.7 b and 2.7 c). If we take a travel distance to Albany of ≈ 400 km and surface winds of ≈ 5 m/s, increasing to, say, 10 m/s at 1000 m a.g., travel times would be between 10 hours and 20 hours. I would expect, then, that TMI plumes should have been widespread across NY State and beyond from the early evening of March 28 on, but not yet touching the ground. TMI plumes starting later in the afternoon and evening with potential temperatures around 280 ° K (Fig. 2.7 b) might have become elevated because of their warmer temperatures, but the next day Albany warmed up to 283 °K (Fig. 2.7 c), enabling the elevated plumes to be mixed down to the surface. This timing would agree with estimated travel times, and with the reported plume appearance near Albany not before March 29, 12.30 E.S.T.

The computed trajectories (Telegadas, 1979) show very nicely the vagaries of the winds and the possible loopings of plume paths in the course of the first few days after time Zero. The author's use of a "transport layer between 300 and 1500 m above terrain" tends to smooth out the strong wind shear across this very layer: Releases near the lower boundary will travel north or northnorthwest (Fig. 6.2), only the higher ones will head to the northeast. Thermodynamic considerations using potential temperature should be added to these trajectories.

My preliminary conclusion is that TMI plumes stagnating over Cumberland County during the night March 28/29 and being mobilized again on March 29, on the approach and passage of the first warm front (chapter 2.4), are not necessarily the source or the only source of Xe-133 appearing at Albany, N. Y. However, the stagnation process itself is beyond doubt.

The numerical model, when fully tested and evaluated, may help to better understand the complicated regional transports, taken together with many more data on concentration hopefully existing. However, the model does have its limits. For example, whereas the model simulates the daily march of temperature very well on March 28, later in the night March 28/29, it cannot develop the very low-lying frontal inversion before the passage of the first warm front, because it wrongly forces the same amount of warm-air advection near the surface as further up. We try to artificially remedy this situation by assuming clear skies (again wrong) and consequent radiational cooling of the surface layer, hoping that the two wrongs will combine to yield a right. Evidently, this technique is less than ideal.

The ARAC Report (Knox et al., 1980), at first sight, promises to afford an interesting comparison of regional models. It makes passing reference to some noteworthy additional meteorological observations, albeit not available before March 31. The MATHEW/ADPIC code makes use of mass-consistent wind fields (see chapter 3 for a critique). It is not clear which meteorological data were actually used. The only plots of plumes shown are for April 1, 1979. The report is almost exclusively concerned with dodging the blame for the organizational and administrative chaos, and trying to establish a rationale for expansion by promises for the future. Its scientific and meteorological contents are practically nil. At the end of this obscure black box, and with omissions even more serious than Woodard's, the authors come up with that one desired number: The "population dose" of 275 person-rem! Both the concept (for a brief critique see chapter 7) and the numerical result are political rather than scientific categories.

7. Near-site Dispersion of TMI plumes Dose Estimates

Distances up to ≈ 10 miles are envisaged in this last part of the treatise. Before going through some proposed szenarios, I must establish a framework for them.

7.1 Releases

There are simply no trustworthy final informations from official sources regarding the quality and quantity of releases. I refer to my chapter 1, regretting that some further work on this topic is not available to me yet. The data resolution of environmental monitoring was far too poor:

- Regular helicopter surveys did not start until March 30, when the hottest plumes were gone. Even then, they failed to cover the area with any degree of completeness, relying on highly arbitrary extrapolations and interpolations and empirical corrections.

- TLD coverage is most unsatisfactory:
  3 out of 16 sectors have no TLD, among them the ESE sector, into which WNW winds are blowing, the most frequent winds at Harrisburg!

Consider, for comparison, that the use of many more measuring sites in much easier terrain still did not suffice to give good model verification in the classical peer reviews (see chapter 5.1). The fundamental critique of TLD's will not be repeated here, except to note that large releases in narrow plumes under stable conditions could easily go undetected, unless the plume happened to cross a TLD straight overhead (Fig. 1.2).

For the plume on the afternoon of March 28, I will use Webb's blowout:

$$Q = 60 \times 10^6 \text{ Ci Xe-133 in 3 hours.}$$

All other szenarios are normalized with respect to the rate of release

$$Q = 1 \times 10^6 \text{ Ci in 1 hour.}$$

This is close to Woodard's largest admitted values ("Release Rate of Noble Gases from TMI-2 ...").

It could well be an underestimate for a number of releases. I am rather unhappy about considering Xe-133 only and the respective dose factors (see further down), knowing that very hot radioactive plumes or puffs must have escaped the first day. One reason is simply convenience of comparison with Woodard's model in meteorological terms. I am not purporting to imitate Woodard's complete statistics. My aim is to contrast my own dispersion szenarios with Woodard's, assuming equal releases. Of course, I have chosen parameters which could be representative of plausible real conditions. In most cases, the reader can easily see how different parameters would change the result. This is, unfortunately, not true if Xe-133 only makes a minor contribution to the mix of nuclides.

7.2 Plume Depletion - Deposition

It is not necessary to include plume depletion on the relatively short near-site trajectories. However, two points are in order:

1. The light rains during the night March 28/29 with totals of about 0.04 inches in the area may have a strong bearing on wet deposition of certain radioactive effluents. Only it appears hopeless to try to understand and describe the physical and chemical transformations within the radioactive plume, before much more has been learned.

2. Dry and wet deposition of gases and particles needs to be studied. Deposits would be extremely helpful witnesses regarding quantity and kind of releases and dispersion properties, but may be hard to identify after 15 years.
   Again, we must await a lot of interdisciplinary search and research. There is no doubt, however, that deposition is even more variable than concentration, being substantially enhanced where forests begin or in the wake region near obstructions (hot spots). Large localized deposition can occur far from a pollution source, and pollution can travel for at least tens of miles with scarcely any dilution (see e. g. Scorer, 1992).

7.3 Dose factors

The paper by Berger (1974) may serve to highlight the complications inherent in beta-ray penetration into tissue, and the fact that extremely "hot" radioisotopes go along with reactor effluents. Progressing from here, the legitimate question arises on which basis official "dose conversion factors" have been obtained. Medical X-ray treatment? Do we understand the interactions of ionizing radiation with human or plant tissue well enough to define them with what is cynically called a "quality factor"? Officially, this "quality factor" = 1, that is, 1 Röntgen = 1 rem for γ-and β-radiation.

I will have to make use of official dose factors for Xe-133

$$F_\gamma = 3.3 \times 10^{-2} \ \frac{mR / hr}{\mu Ci / m^3} \qquad \text{("whole body")}$$

$$F_\beta = 0.25 \ \frac{mR / hr}{\mu Ci / m^3} \qquad \text{(skin and breathing)}$$

(both for submersion in a radioactive cloud), replacing rems by Roentgens to make sure that I interpret them only as a relative measure of danger, in no way accepting the fact that nuclear physics and technology seem to have successfully preemptied this field by promoting official factors. Could we hope to establish realistic dose-effect relationships without, e.g., understanding the indirect damaging effects on the immune system, which may raise the above-quoted official beta-dose conversion factor F_β by a "quality factor" of 10 to 20?

7.4 Szenarios #1: Plume or Puff Impingement

Plumes or puffs released in very stable conditions, impacting on a hill slope (see chapter 4).

For a start, the local terrain around TMI is shown in Fig. 7.1. For each wind direction, there are hills and ridges surmounting effective release heights of $\approx$ 300 ft + some 150 or 200 ft.

Hanna and Strimaitis (1990) describe how a plume extending across both sides of the stagnation streamline splits and wraps around the leading edge of the hill. In the Cinder Cone Butte Experiment, oil plumes

Fig. 7.1:
Local topography around TMI and Harrisburg.
Constructed by pasting together USGS County maps

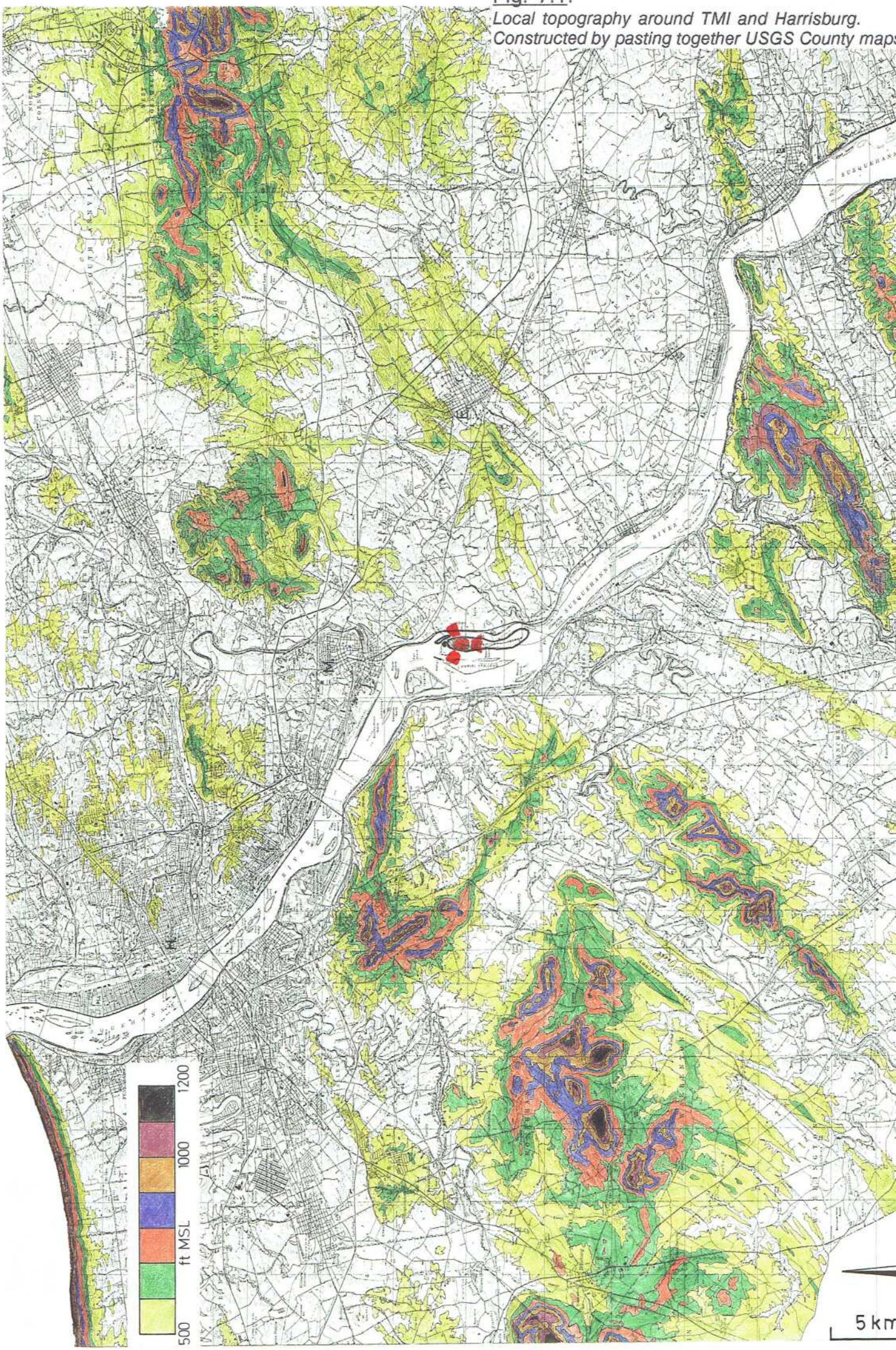

below the "dividing streamline height" would either tend to skirt the hill altogether, or, within a narrow angle from the stagnation streamline, impinge on it, meandering back and forth across the hill face, producing large concentrations within the sampler array on the hill.

Meroney (1990) quotes Snyder's wind tunnel experiment on the same hill, illustrating the high sensitivity of lateral plume movement around the hill against small shifts of the wind direction (Fig. 7.2).

Fig. 7.2:
Angle sensitivity of lateral plume movement around a hill in stratified flow (Snyder, 1988).
Isolines of concentration ——— *for wind direction 117°*
– – – – – *for wind direction 122°*

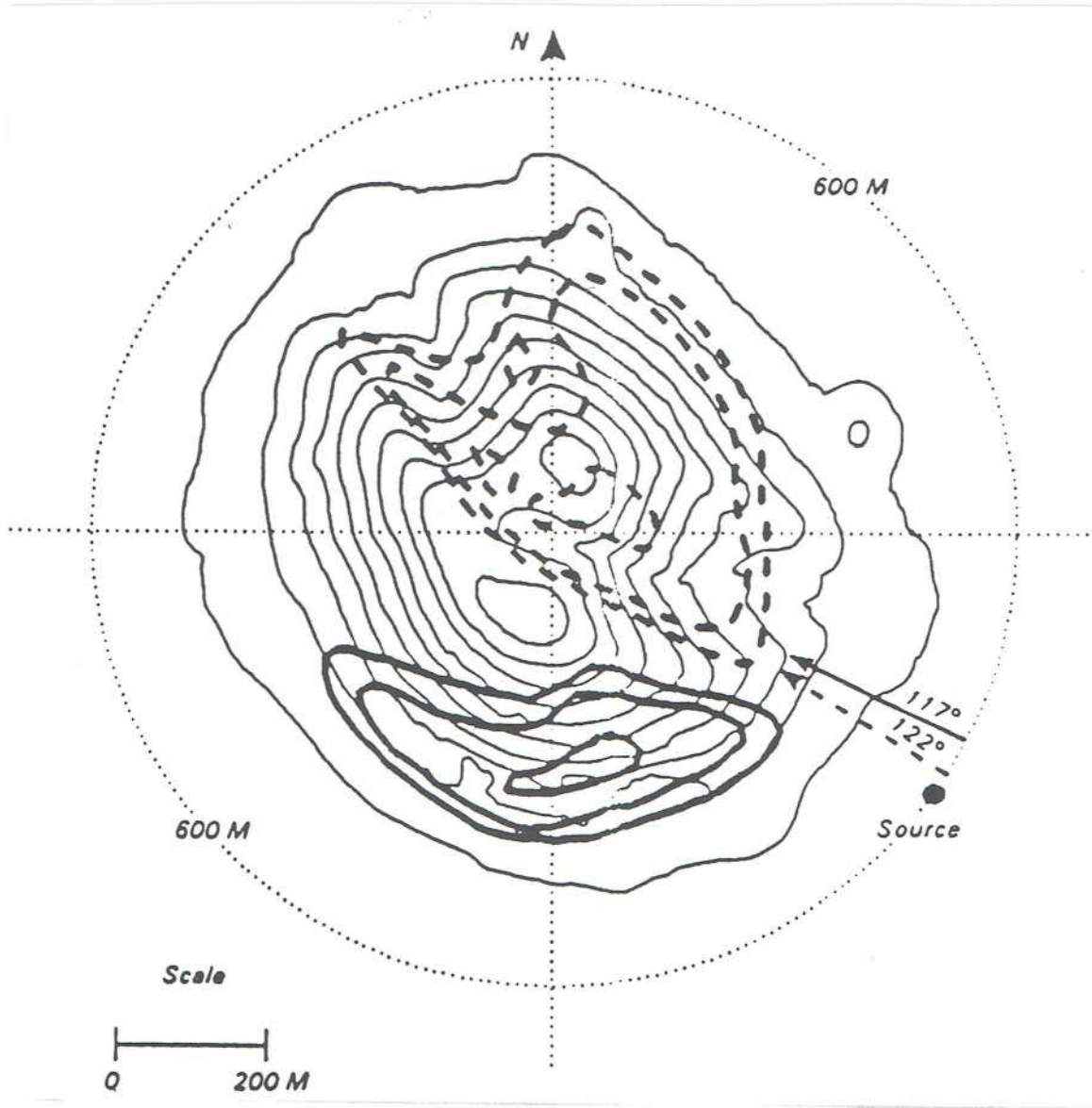

Fig. 7.3 has a plume meander across the face of a hill. Taking wind speed u = 2 m/s, the smaller of the release rates Q as explained above, and lateral and vertical plume dimensions roughly 50 m and 10 m, respectively (see chapter 5.3), not worrying about Gaussian profiles in the plume, we end up with a concentration

$$C \approx 0.3 \frac{Ci}{m^3},$$

and an official β-dose rate of ≈ 70 R/hr.

Remember the factor of 10 to 20 for realistic β-damage and we would plausibly have bridged the gap between some tens or hundreds of "mrems" recorded by TLD's, and the acute symptoms of radiation sickness requiring hundreds of rems. The plume would only have to shed a segment (a wake eddy) staying in a particular sheltered concave place for an hour or so, before being replaced with a fresh gust. This seems more likely than the entire plume drifting alongside the hill for an hour.

What about Woodard? What would his model compute, given the same release hitting a similar hill? I can't be sure, as explained in chapter 5.4, but we can try. Let the hill be several km from TMI. Then, from Turner (1970), for stability class F $\sigma_y \approx 250$ m and $\sigma_z \approx 45$ m. The respective plume dimensions would be $\sqrt{2\pi}\ \sigma_y \approx 625$ m and $\sqrt{2\pi} \cdot \sigma_z \approx$ 110 m roughly, and $C \approx 0.2 \times 10^{-2}$ Ci/m^3 , or at least 100 times lower than my maximum estimate.

Clearly, the result depends critically on how narrow and thin the plume is taken to be. It should come as no surprise that standard stability classes do not cover the kind of extreme events to be expected in this drastically stable synoptic situation (see chapter 2). The standard sigma-values incorporate plume meandering (see chapter 5.2 and 5.3). However, the plume proper can all the same be very narrow and undiluted.

There is a further important consideration: Does the grid resolution used by Woodard force a minimum effective plume dimension or puff size, and if so, how? Woodard states that his fine-mesh polar calculation grid has 64 direction sectors and 52 radial increments ranging from 100 m to more than 5000 m at 50 miles from TMI. This would appear to imply that effective puff size could be no smaller than ≈ (1 km)^2 at, say, 10 km distance.

Fig. 7.3:
Plume impaction szenario.
Plume meandering across a hill face. See text.

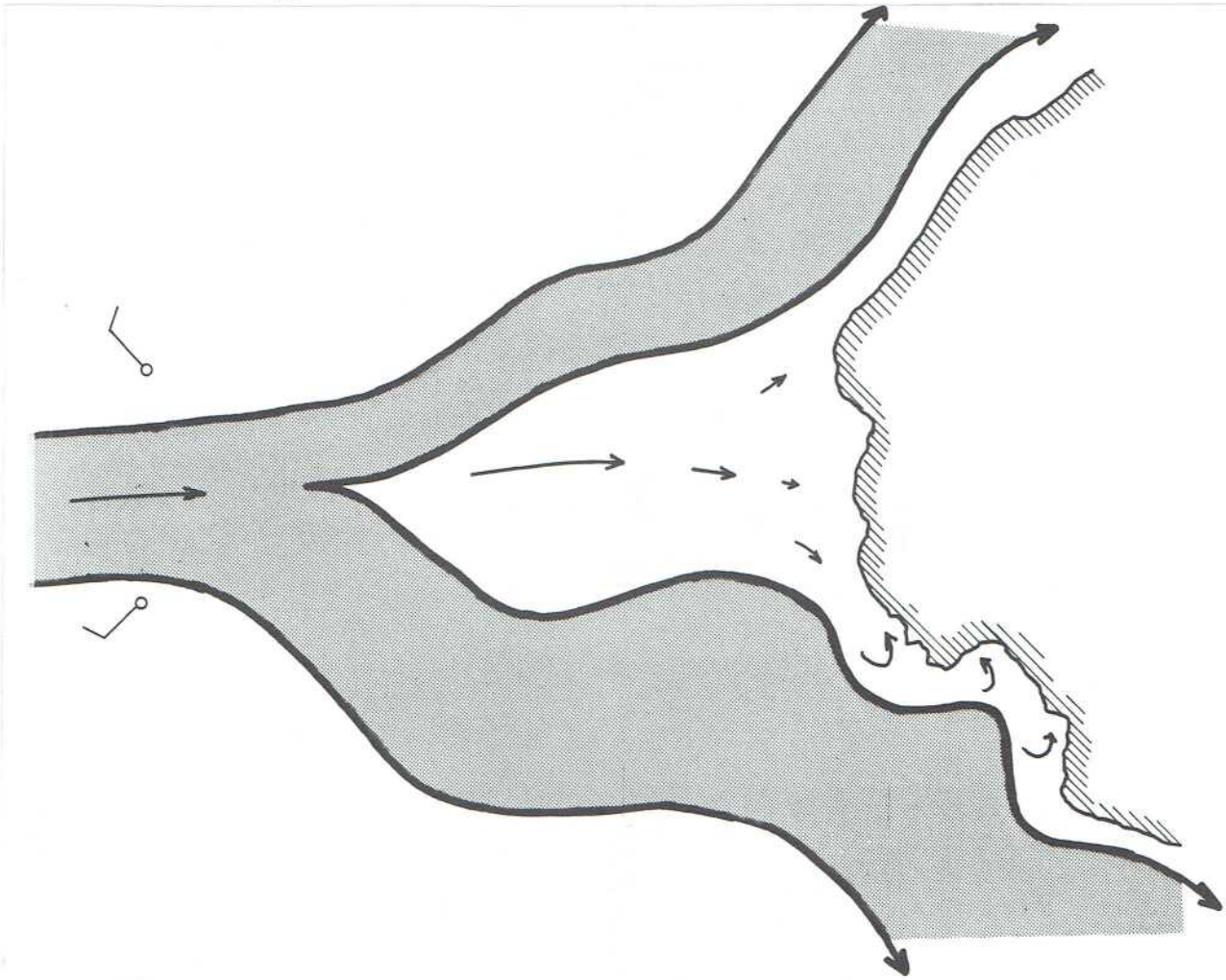

The consequences would be immediately obvious: Concentrations would be more than 100 times lower than in my szenario, depending also on how vertical resolution is treated, and computed β-dose rate would be ≈ 500 mR/hr or lower. Woodard, of course, pretending to know only about γ's, would arrive at numbers of 50 mR/hr or less (note the milli-Roentgens!). Even if the extremely stable category G had been applicable, Woodard, by his enforced averaging, would end up with no higher concentrations and dose rates.

We can only hope that the fact that wind directions and topography data given by Woodard are still resolved in only 16 sectors N, NNE, NE, ENE ... does not mean that his plume segments reflect sector averaging at 22.5°, and that the above-mentioned fine-mesh grid serves only for summing the contributions?

Fig. 7.4:
Puff impaction szenario in variable wind. See text.

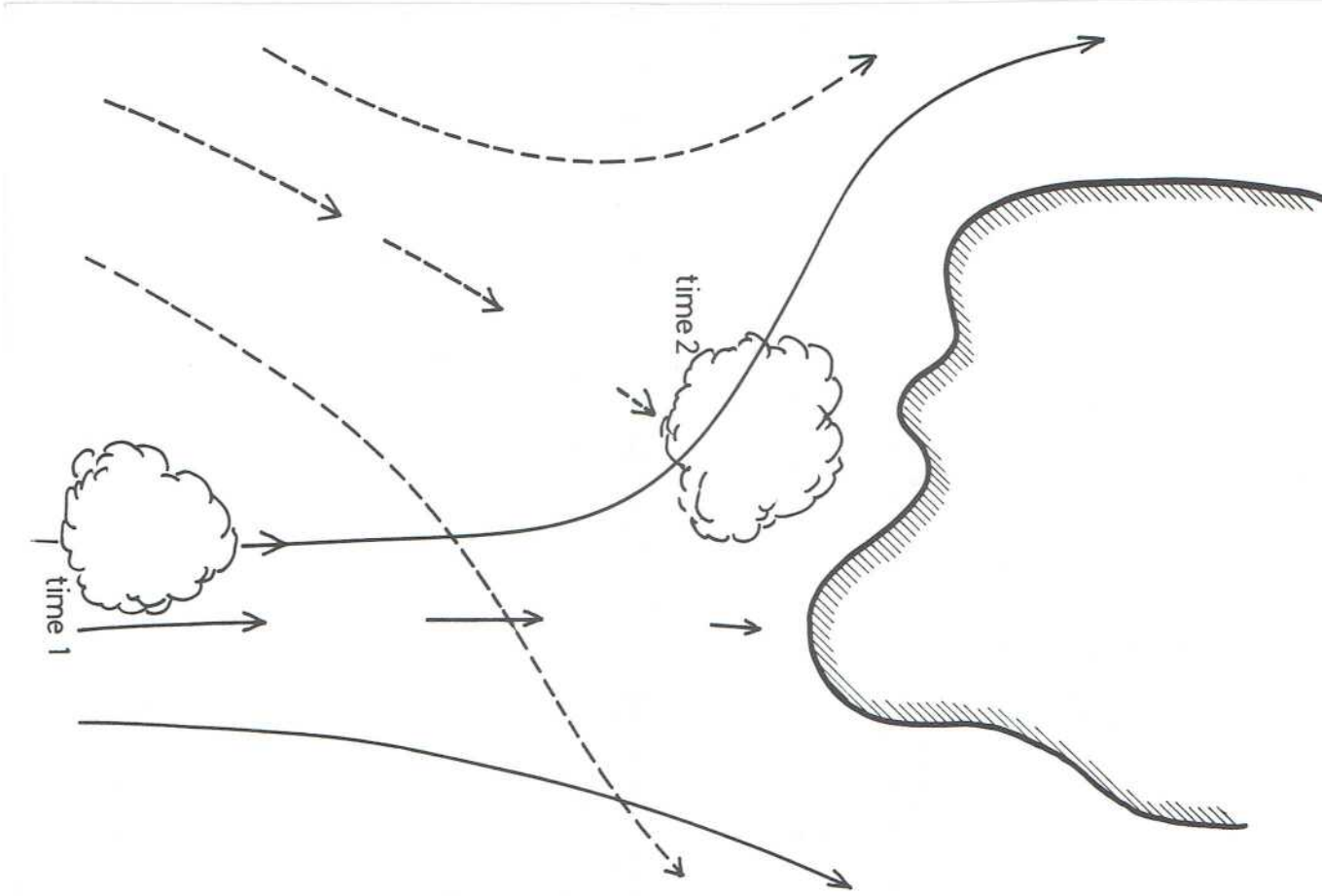

The same szenario can be modified a bit to conform more closely to the puff mode:

Let Q = 250 000 Ci in 15 minutes, and u = 2 m/s = 1.8 km in 15 minutes. At that distance downwind, $\sigma_y \approx 60$ m (stability class F) and $\sigma_z \approx 20$ m. As these are standard values (from Turner, 1970) and as we are quite sure that the vertical plume depth $\sqrt{2\pi}\ \sigma_z$ can be as small as 10 m or smaller in the extreme, we might scale down σ_y accordingly to obtain lateral dimension $\sqrt{2\pi}\ \sigma_y \approx 30$ m.

The extent of this elongated puff ("pencil dispersion") ends up being 1.8 km x ($\frac{1}{2}$ 30 m) x 10 m, and the average concentration C $\approx$ close to 1 Ci/m^3. Let this puff - we may think of it as being broken up into small

segments like the one drawn in Fig. 7 .4 - drift across the countryside and approach a hill, say, left of the stagnation streamline (time 1). A bit later (time 2), the wind might have shifted a little, and the puff would find itself caught on the new stagnation streamline near a concave section of the hill, sheltered from being cleared away by the changing feeble wind currents for some time.

In fact, we can relax the parameters of this szenario by a factor of 3 or 4 (lower release rate Q or not so extremely small dispersion or shorter stagnation time) and still end up with

$$C \approx 0.3 \text{ Ci/m}^3$$

and official β-dose rate $\approx$ 70 R/hr, as before.

Finally, let's pursue a variation on this puff sequence, illustrating the ad-hoc nature of necessary assumptions:

Release time = 1 minute

$Q = 10^6$ Ci/hr = 17 000 Ci in 1 minute.
Travel distance (2 m/s) = 120 m during release
From Turner for stability F:

σ_y (120 m) = 4.8 m
σ_z (120 m) = 2.7 m

As the vertical depth comes out to be $\sqrt{2\pi}\ \sigma_z$ = 6.8 m, we don't need to modify the sigmas.
Puff volume will be $\approx$ 120 m x ($\frac{1}{2}$ 12 m) x 6.8 m $\approx$ 5000 m^3, and average concentration C $\approx$ 3.4 Ci/m^3!

We can now either allow for some dispersion of this horrendous wisp of a plume on its later trajectory, or relax other parameters as shown before, or still accumulate a β-dose of, say, 70 R in 5 minutes only! Who could predict the details of release mode, wind fluctuations during the release and ensuing puff shape and concentration?

Obviously, such quantitative scoping calculations cannot be firm predictions for the hundreds of reasons elaborated in this treatise. Inherent atmospheric variability on top of ill-understood intermittency of releases thwarts any such attempt. The problem is not so much that ad-hoc assumptions are necessary but that Woodard doesn't spell out his different implicit assumptions. Along the earlier line of reasoning,

Woodard's concentrations might be two orders of magnitude or more lower than mine, taking equal releases. Accordingly, the local γ-dose rate, which I have neglected compared to the beta, would essentially be a factor of 100 or a few hundred higher in my szenario. There is another factor of almost ten for the official beta-dose rate, inexcusably forgotten by Woodard, and maybe another factor of 10 to 20 taking into account the real destructive "quality" of the betas.

Incredible as it may seem at first, the apparent huge discrepancy can be explained rationally.

One necessary assumption here is that the releases will not get mixed down into the building wakes. This is plausible in weak winds and very stable conditions. Note that I am not predicting extreme plumes and puffs to impinge on the slopes everywhere, but only occasionally and locally when conditions are right. In other places, effluent concentrations and doses might be lower or far lower, but still highly damaging. Which areas will be affected? This will depend on the prevailing wind direction, but a look at Fig. 2.3 reminds us how variable winds are in a weak-gradient situation. The three measured winds shown are all from fairly well exposed stations along the Susquehanna River Valley; none is from outlying areas, and yet wind variance in space and time is quite substantial. Only the afternoon and early night of March 28 show a semblance of a uniform, slowly changing wind pattern with fair speeds. At all other times (up to March 30), affected areas could only be outlined in a very tentative way. The only firm conclusion is that two major preconceived notions of the Defendants, not spelled out explicitly but adhered to rigidly, do not stand closer scrutiny:

1. Doses inflicted were generally low.
2. Maximum doses occurred very close to TMI, falling off rapidly with distance.

7.5 Szenario #2: Fumigation

Possible example: Goldsboro, morning of March 28,
weak winds from easterly directions (2 m/s)
See Fig. 7.5.

A previously established stable plume at 60 m a.g., stability class F, is being mixed down to the surface in the very early growth stage of the CBL (chapter 5.2).

Plume travel distance 2 to 2.5 km.
σ_y = 70 m, lateral extent $\sqrt{2\pi}\ \sigma_y \approx 170$ m
σ_z doesn't matter.

No downscaling of σ_y because of later mixing (ad hoc).
Then, for a "standard" release Q = 10^6 Ci in 1 hr, the plume over Goldsboro contains

$$\approx 0.8\ \text{Ci/m}^2.$$

Upon being mixed down 60 m, the concentration in the entire shallow column of air will be

$$C \approx 0.014\ \text{Ci/m}^3.$$

Fig. 7.5:
Fumigation szenario (see text)
with possible additional circulations.

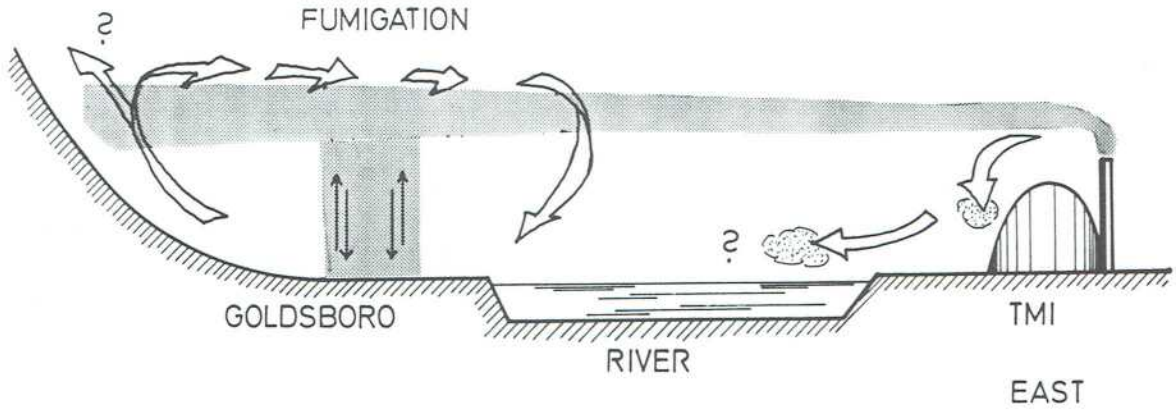

This is a factor of 20 lower than our earlier very ad-hoc extreme puff concentration, but still a factor of almost 10 higher than ground concentrations in an ordinary near-neutral Gaussian plume, given equal release rates. These ratios conform to general experience with fumigation over flat terrain. Absolute values, however, should not be attached to this particular application for many reasons:

- Radioactive releases must have been extremely "hot", making Xe-133 only a minor constituent.

- Plume impaction on the slopes or fumigation along the slopes would make for worse concentrations.

- Thermally driven circulations may develop in slack wind conditions, possibly as indicated in Fig. 7.5.

- Other eddy or wake motions may carry deadly puffs to the ground. On crossing the Susquehanna River, these would undergo only little dilution before hitting Goldsboro.

Fumigation of pre-existing nocturnal stable plumes or puffs down to particular hill sites could well have been a critical process causing very high doses locally in scattered places.

7.6 Szenario #3: Afternoon Blowout, March 28

This major release, at first glance, promises to be associated with the most manageable meteorological conditions, namely a mixed layer ≈ 1200 m deep as shown on the Washington radiosounding (Fig. 2.2), and plausible from the fair weather. This expectation may be fulfilled at around 2 p.m., when the blowout likely started (see Fig. 1.1). Taking the Webb blowout release and the meteorological dispersion factor 0.4 x 10^{-6} s m^{-3} from chapter 1.4 for Middletown, hourly averaged ground concentrations of Xe-133 there might have been

$$C \approx 2 \times 10^{-3} \text{ Ci/m}^3,$$

or roughly two orders of magnitude below our extreme ad-hoc estimates for local impaction on hill slopes. The difference, of course, would be that these lower concentrations and doses would affect a much larger area.

Later in the afternoon, however, the weather frame becomes much more ambiguous:

- Warm-air advection picked up strength, mostly at somewhat higher levels, corresponding to the position of the surface warm fronts still far to the south, but possibly at lower levels, too, in the usual

sporadic, tongue-like manner (see e. g. chapter 2 and the cloudiness in Fig. 2.3). The consequence would be sheetwise stabilization of the lower atmospheric layers. The Washington sounding need not be representative of the Harrisburg area.

- The upward sensible heat flux from the surface, main driving force of turbulent mixing motions in the boundary layer, turns negative quite a bit before sunset, usually between 2 and 4 p.m. The surface layer will begin to cool soon afterward, forming a stable surface inversion and leading the transition from CBL to evening SBL, the least-studied phase of boundary layer development. Turbulence in the boundary layer may drop rather abruptly, with only the wind shear left as a driving force. The cool air will tend to flow downhill and collect in low-lying areas.

- As a lesson from chapters 5.2 and 5.3, we must not think of mixed boundary layers as being all uniform and predictable, much less of a boundary layer in transition, with turbulence settling down and advection dominating. It will be filled with wakes trying to conserve their circulation, and air parcels, once caught up in a wake, will tend to stay there fairly long. I am not in a position to propose detailed flow or eddying patterns. I can, however, illustrate the principles at work with two fairly simple exercises:

a) Plume from TMI heading roughly north or northnorthwest.
Taking a Gaussian plume for demonstration only.

Effective plume cross section = $2\pi \cdot \sigma_y \cdot \sigma_z$ at 5 km distance from TMI (Middletown)
for stability class B = 260×10^4 m^2
for stability class F = 3.2×10^4 m^2.

Thus, even the official stability classes, far from extreme events, span two orders of magnitude between B and F. When Woodard has stability class A, his failure to take account of the mixing height will lead to negligible concentrations at the larger distances.

b) Let the radioactive effluents be discharged into a building wake of size $\approx$ 250 ft (width) x 170 ft (height) x 1000 ft (length) $\approx 10^6$m^3 for 5 minutes, before the entire wake eddy breaks loose and gets swept downstream, possibly in the manner described by Irwin & Smith (see chapter 5.2). Then, average concentration in the eddy would be $\approx$ 1.4

Ci/m^3, and even upon five- or tenfold dilution this would still be enough to inflict heavy doses on better-exposed hilltops.

A combination of factors was likely to have been responsible for the locally very high concentrations and doses apparently due to wisps of this afternoon plume:

- Large releases
- Quasi-continuous plume lasting some hours, i. e. long exposure
- Plume cross section narrowed by mixing height and streakiness (see above)
- Hilltops at just about the effective release height
- Deposition processes reportedly more active in the daytime than at night (average factor ≈ 5?). I don't know whether this is true in our case.

7.7 A last word on population dose

This favourite of all official studies, purporting to characterize an immensely complex and ugly reality with one number, has no merit whatsoever. Remember the spottiness of concentrations and doses, not predicted by any of the officially used models (TMIDOSE, AIRDOSE, ARAC, see also chpt. 6). Remember the fundamental inability of any model to produce correct point forecasts. The models just smear out everything over large areas, but at the same time they fail to account for some of the most important meteorological and biological processes. For compensation, they perform lots of involved integrations. You cannot average out lethal doses with small doses. Babies, children, adults, sick people are all sensitive to radiation in individually different ways. Population dose throws them all in one basket.

Acknowledgements

I deeply appreciate the most helpful cooperation by Prof. R. Steinacker and I acknowledge further consultations with Dr. P. Brunner, Prof. J. Gunckel, Dr. P. Seibert, Dr. D. Heimann and Dr. J. Graf, Mag. M. Lezius, Dr. Chr. Schär, Dr. K. Hinrichsen and, last not least, Dr. R. Webb, who rendered able insight to matters all of which I reconfirmed. I further acknowledge the following well-done jobs:

Data processing:	F.-D. Jäger, B. Siegele
Computer assistance:	F. Pellet
Drawings:	N. Span
Typing:	K. Pfurtscheller
Copying:	Studia

Men and women of history, and many people and friends have taught me and encouraged in me the excitements of life and science, the joys and the burden of critical thinking and, I hope, a sense of truth and justice, for which I consider myself very fortunate.

REFERENCES

Berger, M. J., 1974: Beta-Ray Dose in Tissue-Equivalent Material Immersed in a Radioactive Cloud. Health Physics, Vol. 26, pp. 1 - 12.

Blumen, W., 1990: (ed): Atmospheric Processes over Complex Terrain. Meteorological Monographs, vol. 23, American Meteorological Society, 323 pp.

Carlson, T. N., 1991: Mid-Latitude Weather Systems. Harper Collins Academic, London.

Carruthers, D. J. and J. C. R. Hunt, 1990: Fluid Mechanics of Airflow over Hills: Turbulence, Fluxes and Waves in the Boundary Layer. Chpt. 5 in: Atmospheric Processes over Complex Terrain, (W. Blumen ed.), pp. 83 - 107.

Castro, I. P., and G. L. Marsh, 1983: Stratified flow over three-dimensional ridges. J. Fluid Mech. 135, 261 - 282.

Deardorff, J. W. and G. E. Willis, 1975: A Parameterization of Diffusion into the Mixed Layer. Journal of Applied Meteorology, Vo. 14, pp. 1451 - 1458.

Derbyshire, S. H., 1992: On the Sensitivity of Stable Boundary Layers to Small Slopes and Other Influences. In: Fourth IMA Conference on Stably Stratified Flows - Flow and Dispersion over Topography, Guildford, Surrey, England.

Halitsky, J., 1979: Atmospheric Dispersion Estimates for TMI Unit-2 Vicinity of Plant Structures. Appendix F, TDR-TMI-116, July 1979.

Hanna, S. R. and R. J. Paine, 1989: Hybrid Plume Dispersion Model (HPDM) Development and Evaluation. Journal of Applied Meteorology, Vol. 28, pp. 206 - 224.

Hanna, S. R. and D. G. Strimaitis, 1990: Rugged Terrain Effects on Diffusion. Chpt. 6 in: Atmospheric Processes over Complex Terrain, (W. Blumen, ed.), pp. 109 - 143.

Hanna, S. R., 1992: Effects of data limitations on hopes for improved short-range atmospheric dispersion models. In: DCAR-Workshop, Objectives for Next Generation of Practical Short-Range Atmospheric Dispersion Models, Risø National Laboratory.

Hanna, S. R. and J. C. Chang, 1993: Hybrid Plume Dispersion Model (HPDM) Improvements and Testing at Three Field Sites. Atmospheric Environment, Vo. 27 A, 9, pp. 1491 - 1508.

Hunt, J. C. R. and W. H. Snyder, 1980: Experiments on stably and neutrally stratified flow over a model three-dimensional hill. J. Fluid Mech., 96, pp. 671 - 704.

Hunt, J. C. R., 1985: Diffusion in the Stably Stratified Atmospheric Boundary Layer. Journal of Climate and Applied Meteorology, Vol. 24, pp. 1187 - 1195.

Irwin, J. and M. Smith, 1984: Potentially useful additions to the Rural Model Performance Evaluation. Bull. AMS 65 (6), pp. 559 - 568.

Knox, J. B. et al., 1980: Utilization of the Atmospheric Release Advisory Capability (ARAC) services during and after the Three Mile Island accident. Lawrence Livermore Laboratory, UCRL-52959.

Mason, P. J. and R. I. Sykes, 1979: Flow over an isolated hill of moderate slope. Quart. J. Roy. Meteor. Soc., 105, pp. 385 - 395.

Meroney, R. N., 1990: Fluid Dynamics of Flow over Hills/Mountains - Insights Obtained through Physical Modeling. Chpt. 7 in:Atmospheric Processes over Complex Terrain (W. Blumen, ed.), pp. 145 - 171.

National Meteorological Center, NWS: Surface Analysis, 850 mb Analysis. National Climatic Data Center, Asheville, N. C.

NOAA, 1979: Climatological Data. Vol. 84. National Climatic Center, Asheville, N. C.

Riddle, A. M. and T. B. Staples, 1992: Dispersion of Industrial Gases over Variable Topography. Fourth IMA Conference on Stably Stratified Flows, Guildford, Surrey, England.

Schaer, Chr. and D.R. Durran, 1994: Paper on 3-D flow over a model obstacle, in print (probably Journal of Atm. Sci.). Title not on hand at the moment.

Scorer, R. S., 1978: Environmental Aerodynamics. Ellis Horwood Ltd., 487 pp.

Scorer, R. S., 1992: Deposition of Concentrated Pollution at Large Distance. Atmospheric Environment, Vo. 26 A, 5, pp. 793 - 805.

Slade, D. H., 1968: Meteorology and Atomic Energy, 1968. U. S. Atomic Energy Commission, 445 pp.

Smith, M. E., 1984: Review of the Attributes and Performance of 10 Rural Diffusion Models. Bulletin American Meteorological Society, Vol. 65, 6, pp. 554 - 558.

Smith, R. B. 1989: Hydrostatic Airflow over Mountains. Advances in Geophysics, Vol. 31, pp. 1 - 41.

Snyder, W. H., 1988: Integration of fluid modeling with complex-terrain field studies and model-development efforts. Proceedings Eighth Symposium on Turbulence and Diffusion, San Diego, pp. 189 - 192.

Steinacker, R., 1984: Die luftmassenmäßige Arbeitsweise im regionalen scale. Institut für Meteorologie u. Geophysik d. Univ. Wien, Publik. Nr. 30, Schinze-Preis 1984.

Stull, R. B., 1989: An Introduction to Boundary Layer Meteorology. Kluwer Academic Publishers, 666 pp. (1st edition 1988).

Task Group on Health Physics and Dosimetry, 1979: Report. Sequence of Events pp. 6 - 14. Exhibit H in: Defendants' Reply Brief in Support of their Motion for Summary Judgement.

Taubensee, R. E., 1979: Weather and Circulation of March 1979. Monthly Weather Review 107, 788 - 794.

Telegadas, K., 1979: Estimated low level trajectories originating from Middletown, PA, for the period March 28, 1979 through April 4, 1979. Air Resources Labs., NOAA.

Turner, D. B., 1970: Workbook of Atmospheric Dispersion Estimates. US EPA.

U. S. NRC, 1977: Methods for Estimating Atmospheric Transport and Dispersion of Gaseous Effluents in Routine Releases from Light-Water-Cooled Reactors. Regulatory Guide 1.111, 24 pp.

U. S. Department of Commerce, NOAA, NWS: Aviation Weather Observations. National Climatic Data Center, Asheville, N. C.

Vergeiner, I. and E. Dreiseitl, 1987: Valley Winds and Slope Winds - Observations and Elementary Thoughts. Meteorol. Atmosph. Physics, 36, pp. 264 - 286.

Wagner, A. J., 1979: Weather and Circulation of April 1979. Monthly Weather Review, 107, 948 - 954.

Wahlen, M., et al., 1980: Radioactive Plume from the Three Mile Island Accident: Xenon-133 in Air at a Distance of 375 Kilometers. Science, Vol. 207, pp. 639 - 640.

Webb, R. E., 1993: Analysis of the Three Mile Island Nuclear Accident with respect to the Release of Noble Gas Fission Product Radioactivity into the Atmosphere.

Weil, J. C., 1985: Updating Applied Diffusion Models. Journal of Climate and Applied Meteorology, Vol. 24, 11, pp. 1111 - 1130.

Willis, G. E. and J. W. Deardorff, 1978: A Laboratory Study of Dispersion from an Elevated Source within a Modeled Convective Planetary Boundary Layer. Atmospheric Environment, Vol. 12, pp. 1305 - 1311.

Willis, G. E. and J. W. Deardorff, 1987: Buoyant Plume Dispersion and Inversion Entrapment in and above a Laboratory Mixed Layer. Atmospheric Environment, Vol. 21, 8, pp. 1725 - 1735.

Woodard, K., 1993: Assessment of Offsite Radiation Doses from the TMI Unit 2 Accident (TDR - TMI - 116, July 31, 1979 = "Revision 0"), latest revision dated Jan. 15, 1993 = "exhibit C".

CURRICULUM VITAE

Ignaz Vergeiner, Ph. D.

Born: Dec. 13, 1938 in Austria

Studies:
1957 - 61: Mathematics and Physics, Univ. of Innsbruck, Austria
1961: Teaching Diploma in Math., Physics
1961 - 64: Meteorology and Geophysics, Univ. of Innsbruck
(Prof. Herfried Hoinkes)
1965 - 66: Research Assistant with Prof. E. Reiter, Dept. of Atm. Sci.,
Colorado State Univ., Fort Collins, Colorado, USA
1966 - 67 and 1968 - 1970: Visiting Scientist, National Center for Atm.
Research, Boulder, Colorado, USA, with Dr. D. K. Lilly
1970 (June - Dec.): with Prof. Y. Ogura, Laboratory for Atm. Research,
Univ. of Illinois, Urbana, Ill, USA
Since 1971 at the Institute of Meteorology and Geophysics, Univ. of
Innsbruck, Austria.
1976 (Jan. - March): Guest lecturer, Institut für Geophysikalische
Wissenschaften, Freie Universität Berlin, FRG
1978 (Sept.): Visiting Scientist with Dr. R. Hide, Brit. Met. Office
1978 - 82: project leader: Dynamics of the Valley Wind System
(financed by the Austrian equivalent of Nat. Science Found.)
1983 (July, Aug.): Visiting Scientist, Monash University, Dept. of Maths.,
Clayton, Victoria, Australia.
1985 (Aug.): Invitation to Institute of Geophysics, Univ. of Oslo, and
Geofysisk Institutt, Univ. of Bergen, Norway

1983: Candidate for the Greens (Environmental Party) for federal and
state elections

Increasing concern with the destruction of man and environment and th
interrelated causes and possible remedies.

Areas of research and interest:

- Wave motions in the atmosphere, particularly orographic forcing or
various scales (Föhn)
- Local (thermally induced) circulations
- Limits of computer models
- Energy, Environment and Meteorology

- Local Air Pollution Studies
- Nuclear hazards, solar energy

Lectures (Courses) on:

- Meteorology of Air Pollution
- Dynamics of Alpine Wind Systems
- Numerical Methods in Meteorology and Geophysics
- Statistical Methods in Geophysics
- Meteorological aspects of renewable energy
- Local flows

Innsbruck, June 1994 I. Vergeiner

Selection of scientific publications

The Dynamic Structure of Lee Wave Flow as Obtained from Balloon and Airplane Observations (I. V. and D. K. Lilly). Monthly Weather Review 98, 220 - 232, 1970.

An Operational Linear Lee Wave Model for Arbitrary Basic Flow and Two-Dimensional Topography. Quarterly Journal of the Royal Met. Soc. 97, 30 - 60, 1971.

Comments on: "The Chinook at Calgary (Canada)" by W. A. R. Brinkmann. Archiv f. Met., Geophysik u. Biokl. Ser. B,19, 339 - 341, 1971.

A Numerical Shallow-Fluid Model Including Orography with a Variable Grid. (I. V. and Y. Ogura). Journal of Atm. Sci. 29 (2), 270 - 284, 1972.

A Numerical Model of Three-Dimensional Mountain-Induced Gravity Wave Flow. Rivista Italiana di Geofisica (Proceedings of the XIIIth Internat. Meeting on Alpine Meteorology, Saint-Vincent (Aosta), Sept. 1974), Vol. I (Speciale), Juni 1975, pp. 15 - 31.

Föhn- und Leewellenströmung in einem dreidimensionalen numerischen Modell. Berichte des Naturwiss.-Medizinischen Vereins Innsbruck, Okt. 1976, Bd. 63, pp. 11 - 56.

Inversionslagen in Innsbruck (I. Vergeiner, E. Dreiseitl, H. Feichter u. H. Pümpel). Wetter und Leben 30, 69 - 86, 1978.

Foehn flow in the Alps - three-dimensional numerical simulations on the small- and meso-scale. Veröffentlichungen der ZA (Proc. 14th Internat. Meeting on Alpine Meteorology, Rauris, Sept. 1976), 1978, Zentralanstalt f. Met. und Geodynamik Wien, Heft 31, 37 pp.

Eine energetische Theorie der Hangwinde. ITAM Berchtesgaden 1982. DWD Selbstverlag, pp. 189 - 191. Translated into English by D. Whiteman.

The South Foehn Case 4/5 May 1982: Fine-scale pressure and wind analyses in the Inntal and Wipptal (I. Vergeiner, R. Steinacker, E. Dreiseitl). GARP-ALPEX-Public. No. 7, WMO Geneva, Dec. 1982.

Dynamik Alpiner Windsysteme. Bericht zum Forschungsprojekt 3556, Fonds zur Förderung der wiss. Forschung, 129 S., Juni 1983, (gem. m. E. Dreiseitl).

The Thermal Structure of the Inn Valley Atmosphere. (U. Nickus und I. Vergeiner). Archiv Met. Geophys. Bioklim. Ser. A, 33, 199 - 215, 1984.

Dynamics of Katabatic Winds in Colorado's Brush Creek Valley (I. Vergeiner, E. Dreiseitl, C. D. Whiteman), JAS 44 (1), 1987.

An Elementary Valley Wind Model, Special ALPEX issue of: Meteorology and Atm. Physics, 36, 255 - 263 (1987).

Valley Winds and Slope Winds; Observations and Elementary Thoughts (I. Vergeiner and E. Dreiseitl), Special ALPEX issue of: Meteorology and Atm. Physics, 36, 264 - 286 (1987).

Meteorologische Studie über den Zusammenhang zwischen Emissionen der Wiederaufarbeitungsanlage Wackersdorf, Bayern, und den dadurch verursachten Imissionen in Österreich. Zentralanstalt für Meteorologie und Geodynamik, Mai 1989 (im Auftrag des Bundeskanzleramtes). Autoren: H. Kolb, P. Seibert, I. Vergeiner, R. Steinacker, H. Pichler, R. Perels u. a.

Comments on: "Large-Eddy Simulation of the up-slope Boundary Layer" by U. Schumann (QJRMS 1990, 116, 637 - 670). QJRMS 117 (1991, 1371 - 1372).

Various treatises on transport, dispersion and deposition of air pollutants in hilly and mountainous terrain for specific industrial sites and incinerating plants (in German).